

# Gas-Phase Formation of C<sub>5</sub>H<sub>6</sub> Isomers via the Crossed Molecular Beam Reaction of the Methylidyne Radical (CH; X<sup>2</sup>II) with 1,2-Butadiene (CH<sub>3</sub>CHCCH<sub>2</sub>; X<sup>1</sup>A')

Published as part of *The Journal of Physical Chemistry virtual special issue "Cheuk-Yiu Ng Festschrift"*.

Chao He,<sup>⊥</sup> Anatoliy A. Nikolayev,<sup>⊥</sup> Long Zhao, Aaron M. Thomas, Srinivas Doddipatla, Galiya R. Galimova, Valeriy N. Azyazov, Alexander M. Mebel,\* and Ralf I. Kaiser\*



Cite This: *J. Phys. Chem. A* 2021, 125, 126–138



Read Online

ACCESS |



Metrics & More

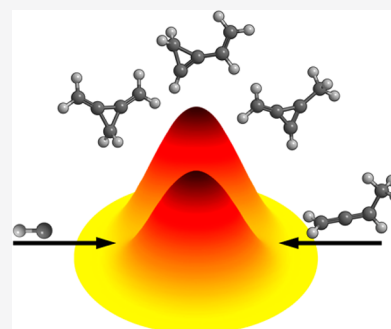


Article Recommendations



Supporting Information

**ABSTRACT:** The bimolecular gas-phase reaction of the methylidyne radical (CH; X<sup>2</sup>II) with 1,2-butadiene (CH<sub>2</sub>CCHCH<sub>3</sub>; X<sup>1</sup>A') was investigated at a collision energy of 20.6 kJ mol<sup>-1</sup> under single collision conditions. Combining our laboratory data with high-level electronic structure calculations, we reveal that this bimolecular reaction proceeds through the barrierless addition of the methylidyne radical to the carbon–carbon double bonds of 1,2-butadiene leading to doublet C<sub>5</sub>H<sub>7</sub> intermediates. These collision adducts undergo a nonstatistical unimolecular decomposition through atomic hydrogen elimination to at least the cyclic 1-vinyl-cyclopropene (p5/p26), 1-methyl-3-methylenecyclopropene (p28), and 1,2-bis(methylene)cyclopropane (p29) in overall exoergic reactions. The barrierless nature of this bimolecular reaction suggests that these cyclic C<sub>5</sub>H<sub>6</sub> isomers might be viable targets to be searched for in cold molecular clouds like TMC-1.



## 1. INTRODUCTION

The understanding of the formation mechanisms of polycyclic aromatic hydrocarbons (PAHs) has attracted interest from the combustion science and astrochemistry communities predominantly due to the crucial role of PAH-like species in combustion processes and in the interstellar medium (ISM).<sup>1–7</sup> In deep space, spectroscopic features of PAH-related species such as cations, (de)hydrogenated PAHs, anions, nitrogen-substituted PAHs, and possibly protonated counterparts have been inferred in the ultraviolet (200–400 nm) and the infrared (3–20 μm) regions via the diffuse interstellar bands (DIBs) and unidentified infrared (UIRs) bands.<sup>2,8</sup> These spectroscopic searches propose that PAHs along with their derivatives may contribute up to 20% to the interstellar carbon budget; furthermore, PAH-like species are considered as key precursors leading eventually to the synthesis of carbonaceous nanoparticles (“interstellar dust”).<sup>9</sup> In terrestrial environments, PAHs are considered as toxic byproducts in the incomplete combustion of fossil fuel, coals, and biomass. This causes air and marine pollution eventually resulting in carcinogenic, mutagenic, and teratogenic effects.<sup>10–12</sup> Therefore, the exploration of the fundamental reaction pathways leading to a synthesis of PAHs and their precursors in extreme environments is important to better understand the carbon chemistry in terrestrial environments and deep space such as cold molecular clouds like TMC-1<sup>13</sup> and the dying carbon stars like IRC+10216.<sup>14–23</sup>

Resonantly stabilized free radicals (RSFRs) such as propargyl (HCCCH<sub>2</sub>), 1,3-butadienyl (*i*-C<sub>4</sub>H<sub>5</sub>), and cyclopentadienyl (*c*-C<sub>5</sub>H<sub>5</sub>) have been hypothesized to promote PAH formation in high temperature combustion flames of typically 1200–1500 K.<sup>24–26</sup> Considering the cyclopentadienyl (*c*-C<sub>5</sub>H<sub>5</sub>) radical, extensive experimental and kinetic modeling studies reveal that the reactions of *c*-C<sub>5</sub>H<sub>5</sub> with methyl (CH<sub>3</sub>), acetylene (C<sub>2</sub>H<sub>2</sub>), propargyl (HCCCH<sub>2</sub>), and *c*-C<sub>5</sub>H<sub>5</sub> radical could lead to benzene (C<sub>6</sub>H<sub>6</sub>), the tropylium radical (*c*-C<sub>7</sub>H<sub>7</sub>), styrene (C<sub>8</sub>H<sub>8</sub>), and naphthalene (C<sub>10</sub>H<sub>8</sub>), respectively.<sup>27–36</sup> This interest resulted in the exploration of the reaction of the *c*-C<sub>5</sub>H<sub>5</sub> radical with methyl (CH<sub>3</sub>) computationally on the C<sub>6</sub>H<sub>8</sub> potential energy surface (PES) utilizing quantum chemical BAC-MP4 and BAC-MP2 methods<sup>27</sup> as well as the ab initio G2M(rcc,MP2) and B3LYP/6-311G(d,p) levels of theory by Moskaleva et al.<sup>28</sup> These studies proposed that the methylcyclopentadiene intermediate (C<sub>5</sub>H<sub>5</sub>CH<sub>3</sub>) might be formed via addition of the methyl (CH<sub>3</sub>) radical to the ring system eventually followed by two consecutive atomic hydrogen eliminations to form fulvene, which then undergoes

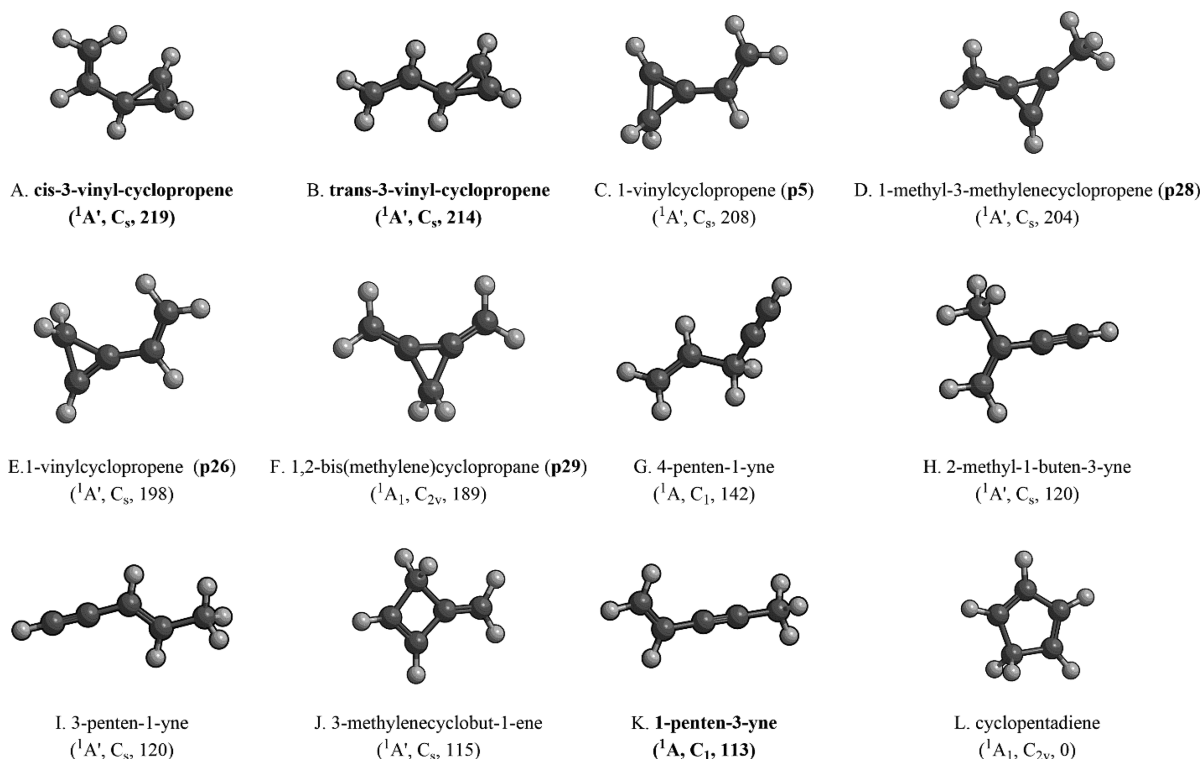
**Received:** September 25, 2020

**Revised:** December 18, 2020

**Published:** January 5, 2021



Scheme 1. Geometries of Selected C<sub>5</sub>H<sub>6</sub> Isomers along with Their Point Groups and Energies (kJ mol<sup>-1</sup>) Relative to the Lowest Energy Isomer Cyclopentadiene<sup>a</sup>



<sup>a</sup>Isomers detected under single collision conditions in crossed molecular beam experiments are denoted in bold.

hydrogen atom-assisted isomerization to benzene (C<sub>6</sub>H<sub>6</sub>).<sup>27,28</sup> Fascella et al. proposed that a rapid reaction pathway may proceed between *c*-C<sub>5</sub>H<sub>5</sub> and acetylene (C<sub>2</sub>H<sub>2</sub>) leading to the tropyli radical (*c*-C<sub>7</sub>H<sub>7</sub>);<sup>29</sup> the existence of this radical was confirmed in time- and isomer-resolved experiments in the acetylene - *c*-C<sub>5</sub>H<sub>5</sub> system below 1000 K.<sup>30</sup> Indene (C<sub>9</sub>H<sub>8</sub>) along with atomic hydrogen might be formed in a successive reaction of the tropyli radical (*c*-C<sub>7</sub>H<sub>7</sub>) with acetylene (C<sub>2</sub>H<sub>2</sub>).<sup>29</sup> Sharma and co-workers developed a chemical kinetics model for the hexadiene-doped methane flames and explored the C<sub>8</sub>H<sub>8</sub> PES using quantum chemistry (CBS-QB3) calculations considering the recombination of *c*-C<sub>5</sub>H<sub>5</sub> and propargyl (HCCCH<sub>2</sub>) leading to styrene (C<sub>8</sub>H<sub>8</sub>).<sup>31</sup> The simplest PAH—naphthalene (C<sub>10</sub>H<sub>8</sub>)—was proposed to be synthesized through the self-recombination of *c*-C<sub>5</sub>H<sub>5</sub> radicals in hydrocarbon flames along with hydrogen atom shifts and two successive hydrogen losses.<sup>32–36</sup>

However, until now, the formation pathway(s) to cyclopentadiene (*c*-C<sub>5</sub>H<sub>6</sub>)—a potential precursor to the cyclopentadienyl radical (*c*-C<sub>5</sub>H<sub>5</sub>)—together with its structural isomers in combustion flames has not been fully explored (Scheme 1). These C<sub>5</sub>H<sub>6</sub> isomers can be classified as (i) isomers carrying a three-membered ring (A–F), (ii) acyclic isomers (G, H, I, K), (iii) four-membered ring isomers (J), and (iv) cyclic isomers with a five-membered ring (L). The chemistry of cyclopropene derivatives (A–F) has drawn substantial interest considering the high ring strain energy of 222 kJ mol<sup>-1</sup>.<sup>37,38</sup> 1-Vinylcyclopropene (C, E) is extremely reactive, even at 195 K; this molecule was first synthesized via dehydrochlorination of chlorovinylcyclopropane.<sup>39</sup> Bolch and co-workers isolated 1,2-bis(methylene)cyclopropane (F) through gas chromatography.<sup>40</sup> Hansen et al. performed a

systematic investigation of the nature of C<sub>5</sub>H<sub>x</sub> species in rich flames fueled by allene (H<sub>2</sub>CCCH<sub>2</sub>), propyne (CH<sub>3</sub>CCH), cyclopentene ((CH<sub>2</sub>)<sub>3</sub>(CH)<sub>2</sub>), and benzene (C<sub>6</sub>H<sub>6</sub>).<sup>41</sup> The most stable C<sub>5</sub>H<sub>6</sub> isomer cyclopentadiene (L) was confirmed to be the dominating C<sub>5</sub>H<sub>6</sub> isomer; the four-membered cyclic isomer 3-methylenecyclobut-1-ene (J) could not be detected.<sup>41</sup> Besides hydrocarbon flames, C<sub>5</sub>H<sub>6</sub> isomers can also be formed in bimolecular reactions.<sup>42–44</sup> Li et al. computed the C<sub>5</sub>H<sub>7</sub> PES exploiting the hybrid density functional B3LYP/CBSB7 level of theory via the reaction of the ethynyl (C<sub>2</sub>H) radical with propene (C<sub>3</sub>H<sub>6</sub>).<sup>42</sup> Formation of the atomic hydrogen emission product, 2-methyl-1-buten-3-yne (H), was initiated through an ethynyl (C<sub>2</sub>H) addition to the carbon–carbon double bond of propene (C<sub>3</sub>H<sub>6</sub>).<sup>42</sup> At higher temperature and collision energies, 3-penten-1-yne (I) + H and 4-penten-1-yne (G) + H are likely products.<sup>42</sup> Crossed molecular beams studies of the 1-propynyl radical (H<sub>3</sub>CCC) with ethylene (C<sub>2</sub>H<sub>4</sub>) revealed the barrierless gas-phase synthesis of distinct C<sub>5</sub>H<sub>6</sub> isomers.<sup>43</sup> The 1-propynyl radical (H<sub>3</sub>CCC) was found to add barrierless to the double bond of ethylene (C<sub>2</sub>H<sub>4</sub>) leading to a long-lived C<sub>5</sub>H<sub>7</sub> complex(es) ultimately forming 1-penten-3-yne (K) along with the atomic hydrogen solely from the ethylene reactant.<sup>43</sup> Furthermore, the methyldiyne radical (CH) plus 1,3-butadiene (CH<sub>2</sub>CHCHCH<sub>2</sub>) reaction was initiated by addition of the CH radical to one of the terminal carbon atom and/or carbon–carbon double bond of 1,3-butadiene without entrance barrier; this reaction resulted in the preparation of three-membered ring products *cis*- and *trans*-3-vinyl-cyclopropene (A, B).<sup>44</sup> However, none of these isomers could have been identified in the interstellar medium so far due to the low dipole moments. Tagging these C<sub>5</sub>H<sub>6</sub> hydrocarbons with cyano groups leads to organics with

**Table 1. Peak Velocities ( $v_p$ ) and Speed Ratios ( $S$ ) of the Methylidyne (CH) Radical, and 1,2-Butadiene ( $\text{CH}_2\text{CCHCH}_3$ ) along with the Corresponding Collision Energy ( $E_C$ ) and Center-of-Mass Angle ( $\Theta_{\text{CM}}$ ) for the CH + 1,2-Butadiene Reaction**

beam	$v_p$ (m s $^{-1}$ )	$S$	$E_C$ (kJ mol $^{-1}$ )	$\Theta_{\text{CM}}$ (deg)
CH ( $X^2\Pi$ )	1827 $\pm$ 15	12.0 $\pm$ 1.2		
$\text{CH}_2\text{CCHCH}_3$ ( $X^1A'$ )	777 $\pm$ 12	9.5 $\pm$ 0.3	20.6 $\pm$ 0.4	60.5 $\pm$ 0.3

significant dipole moments of at least 3 D.<sup>45</sup> This approach has been carried out successfully through the detection of cyanoallene (from allene) and cyanobenzene (from benzene) formed via the barrier-less neutral–neutral reactions of the cyano radical with the corresponding hydrocarbons in the cold molecular cloud TMC-1.<sup>45–50</sup>

Considering that the aforementioned studies on the formation of distinct  $\text{C}_5\text{H}_6$  isomers were dominated by kinetic modeling and ab initio calculation, it is obvious that reaction dynamics studies under single collision conditions are desirable to elucidate the preparation and reaction channels leading to  $\text{C}_5\text{H}_6$  isomers. Here, we report the results of the bimolecular reactions of the methylidyne radical (CH) with 1,2-butadiene ( $\text{CH}_2\text{CCHCH}_3$ ). By merging the experimental data with electronic structure calculations on the  $\text{C}_5\text{H}_6$  and  $\text{C}_5\text{H}_7$  PES, we propose that 1-vinyl-cyclopropene, 1-methyl-3-methylene-cyclopropene, and 1,2-bis(methylene)cyclopropane along with atomic hydrogen are formed via entrance-barrierless, complex forming elementary reactions under single collision conditions. These experimental conditions exclude successive reactions and in particular hydrogen-assisted isomerization processes that would alter the initial reaction products.<sup>51–53</sup>

## 2. EXPERIMENTAL AND COMPUTATIONAL METHODS

**2.1. Experimental Methods.** The methylidyne (CH;  $X^2\Pi$ ) radical reaction with 1,2-butadiene ( $\text{CH}_2\text{CCHCH}_3$ ;  $X^1A'$ ) was conducted under single collision conditions using a crossed molecular beams machine at the University of Hawaii.<sup>54</sup> In the primary source chamber, the pulsed methylidyne molecular beam was formed via photodissociation (COMPex 110, Coherent, Inc.; 248 nm; 30 Hz) of bromoform ( $\text{CHBr}_3$ , Aldrich Chemistry,  $\geq 99\%$ ) seeded in helium (99.9999%; AirGas) at fractions of 0.12% at a backing pressure of 2.2 atm.<sup>20,55</sup> The methylidyne beam passed a skimmer and was velocity selected by a four-slot chopper wheel yielding a peak velocity  $v_p$  of 1827  $\pm$  15 m s $^{-1}$  and speed ratio  $S$  of 12.0  $\pm$  1.2. The rotational temperature of the methylidyne radicals were determined to be 14  $\pm$  1 K via laser-induced fluorescence (LIF).<sup>56</sup> The pulsed (60 Hz) supersonic beam of the 1,2-butadiene reactant was generated in the secondary source chamber with  $v_p$  of 777  $\pm$  12 m s $^{-1}$  and  $S$  of 9.5  $\pm$  0.3; the 1,2-butadiene molecular beam crossed perpendicularly with the CH radical beam at a collision energy  $E_C$  of 20.6  $\pm$  0.4 kJ mol $^{-1}$  and a center of mass (CM) angle  $\Theta_{\text{CM}}$  of 60.5  $\pm$  0.3°. Each supersonic beam was produced via a piezoelectric pulse valve, which was operated at a repetition rate of 60 Hz, a pulse width of 80  $\mu\text{s}$ , and a peak voltage of  $-400$  V. The secondary pulsed valve was triggered 90  $\mu\text{s}$  prior to the primary pulsed valve to account for the distinct velocities and nozzle-to-skimmer distances thus allowing the best overlap and hence highest reactive scattering signal of the methylidyne radicals with 1,2-butadiene. Peak velocities and speed ratios for the reactants along with the corresponding collision energies and center-of-mass angles are summarized in Table 1.

The detector consists of a Brink-type ionizer,<sup>57</sup> a quadrupole mass spectrometer (QMS), and a Daly type ion counter<sup>58</sup> housed within a triply differentially pumped chamber reaching an ultimate pressure of  $6 \times 10^{-12}$  Torr. This assembly is rotatable in the plane defined by both supersonic beams. The neutral reaction products entering the detector are ionized via electron impact ionization (80 eV, 2 mA),<sup>57</sup> then filtered according to their mass-to-charge ratios ( $m/z$ ) through a QMS (Extrel; QC 150) operated with a 2.1 MHz oscillator, and ultimately detected by a Daly type ion counter.<sup>58</sup> Time-of-flight (TOF) spectra were recorded at laboratory (LAB) angles in the range of  $0^\circ \leq \Theta \leq 69^\circ$  with respect to the methylidyne beam ( $\Theta = 0^\circ$ ). For the data analysis, the TOF spectra were integrated and normalized to obtain the product angular distribution in the LAB frame. A forward-convolution routine was used to fit the laboratory data; this procedure represents an iterative method exploiting a user-defined center-of-mass (CM) translational energy  $P(E_T)$  and angular  $T(\theta)$  flux distributions; the  $T(\theta)$  is defined as a sum of up to five Legendre polynomials, whereas a user defined translational energy distribution  $P(E_T)$  can be defined by four input parameters.<sup>59,60</sup> These functions are varied iteratively until best fits of the TOF data and angular distribution are achieved.<sup>61,62</sup> These functions define the reactive differential cross section  $I(u, \theta) \sim P(u) \times T(\theta)$  with the center-of-mass velocity  $u$ .<sup>59,60,63–65</sup> The error ranges of the  $P(E_T)$  and  $T(\theta)$  functions are determined within  $1\sigma$  limits of the errors in the corresponding laboratory angular distribution, velocity spreads, and beam velocities, while maintaining a good fit of the laboratory TOF spectra.

**2.2. Computational Methods.** Geometries of various species on the  $\text{C}_5\text{H}_7$  potential energy surface (PES) accessed by the CH + 1,2-butadiene reaction were optimized employing the B3LYP exchange correlation functional within density functional theory<sup>66,67</sup> and using the 6-311G(d,p) basis set. Then, vibrational frequencies for all optimized structures were calculated at the same B3LYP/6-311G(d,p) level of theory. The frequencies were utilized to characterize these structures as local minima or transition states, to evaluate zero-point vibrational energy corrections (ZPE), and in rate constant calculations. Single-point energies for each optimized structure were rectified using the explicitly correlated coupled clusters method with single and double excitations with perturbative treatment of triple excitations, CCSD(T)-F12,<sup>68,69</sup> using correlation-consistent Dunning's cc-pVTZ-f12 basis set.<sup>70,71</sup> The anticipated accuracy of the CCSD(T)-F12/cc-pVTZ-f12//B3LYP/6-311G(d,p) + ZPE(B3LYP/6-311G(d,p)) results is typically within 4 kJ mol $^{-1}$  or better.<sup>72</sup> The electronic structure calculations employed the GAUSSIAN 09<sup>73</sup> and MOLPRO 2010<sup>70</sup> quantum chemistry software codes. Energy-dependent rate constants for the variety of unimolecular reactions occurring on the  $\text{C}_5\text{H}_7$  surface after the initial bimolecular association step were evaluated within Rice–Ramsperger–Kassel–Marcus (RRKM) theory.<sup>74–76</sup> The internal energy dependent version of the RRKM approach was utilized within the harmonic approximation using our own

code Unimol<sup>77</sup> for multiwell and multichannel unimolecular reactions taking place under single-collision conditions.<sup>78</sup> In this case, the available internal energy is taken as the sum of the collision and chemical activation energies. The calculations take into account only one energy level because no collisional activation/deactivation can occur in crossed molecular beams. Finally, RRKM rate constants are used in product branching ratios calculations within steady-state approximation.

### 3. RESULTS

**3.1. Laboratory Frame.** The reactive scattering signal for the reaction of the methylidyne radical (CH; X<sup>2</sup>Π) with 1,2-butadiene (CH<sub>3</sub>CHCCH<sub>2</sub>; X<sup>1</sup>A') was scanned at mass to charge ratios (*m/z*) of 67, 66, and 65. These TOF spectra were found to be superimposable after scaling, indicating that ion counts at *m/z* = 67, 66, and 65 originate from the same reaction channel, i.e., the formation of C<sub>5</sub>H<sub>6</sub> isomers via the reaction CH (13 amu) + C<sub>4</sub>H<sub>6</sub> (54 amu) → C<sub>5</sub>H<sub>6</sub> (66 amu) + H (1 amu). Ion counts at *m/z* = 65 (C<sub>5</sub>H<sub>5</sub><sup>+</sup>) could be connected to dissociative electron impact ionization of the *m/z* = 66 (C<sub>5</sub>H<sub>6</sub><sup>+</sup>) parent product(s); the signal at *m/z* = 67 (<sup>13</sup>CC<sub>4</sub>H<sub>6</sub><sup>+</sup>) arose from the natural abundance of carbon atom isotopes leading to <sup>13</sup>CC<sub>4</sub>H<sub>6</sub> with the signal accumulated at a level of 5 ± 3%. Since the ion counts of the parent ion *m/z* = 66 (C<sub>5</sub>H<sub>6</sub><sup>+</sup>) were collected only at a level of 19 ± 3% compared to the fragment ion *m/z* = 65 (C<sub>5</sub>H<sub>5</sub><sup>+</sup>), the TOF spectra were acquired at the best signal-to-noise ratio at *m/z* = 65 (C<sub>5</sub>H<sub>5</sub><sup>+</sup>). The resulting TOFs were then normalized with respect to the center-of-mass angle and integrated to yield the laboratory angular distribution (LAD; Figure 1); this distribution is nearly symmetric around Θ<sub>CM</sub> and spans the angular range from 40.25° to 67.75° in the laboratory frame. This result indicates that the reaction of the methylidyne radical with 1,2-butadiene likely proceeds via indirect scattering dynamics through C<sub>5</sub>H<sub>7</sub> reaction intermediate(s) ultimately dissociating to C<sub>5</sub>H<sub>6</sub> by emitting atomic hydrogen. The CH<sub>3</sub>/C<sub>2</sub>H<sub>3</sub>/C<sub>3</sub>H<sub>3</sub>/C<sub>3</sub>H<sub>5</sub> loss channels, which form C<sub>4</sub>H<sub>4</sub>/C<sub>3</sub>H<sub>4</sub>/C<sub>2</sub>H<sub>4</sub>/C<sub>2</sub>H<sub>2</sub> products cannot be probed in the present experiment due to the background counts of CH<sub>3</sub><sup>+</sup>, C<sub>2</sub>H<sub>2</sub><sup>+</sup>, C<sub>2</sub>H<sub>3</sub><sup>+</sup>, C<sub>2</sub>H<sub>4</sub><sup>+</sup>, C<sub>3</sub>H<sub>3</sub><sup>+</sup>, C<sub>3</sub>H<sub>4</sub><sup>+</sup>, C<sub>3</sub>H<sub>5</sub><sup>+</sup>, and C<sub>4</sub>H<sub>4</sub><sup>+</sup> species stemming from dissociative electron impact ionization of the 1,2-butadiene reactant.

**3.2. Center-of-Mass Frame.** For the CH + 1,2-butadiene reaction, the TOF spectra and LAD (Figure 1) can be fit via a single reaction channel CH (13 amu) + C<sub>4</sub>H<sub>6</sub> (54 amu) → C<sub>5</sub>H<sub>6</sub> (66 amu) + H (1 amu). The resulting CM translational energy *P*(*E*<sub>T</sub>) and angular *T*(θ) flux distributions are shown in Figure 2. The hatched areas of the *P*(*E*<sub>T</sub>) and *T*(θ) represent the error limits determined within the 1σ error limits of the LAD. The maximum energy *E*<sub>max</sub> of the CM translational energy distribution *P*(*E*<sub>T</sub>) (Figure 2), the collision energy (*E*<sub>C</sub>), and the reaction energy (Δ<sub>r</sub>*G*) are connected via *E*<sub>max</sub> = *E*<sub>C</sub> - Δ<sub>r</sub>*G* for those molecules born without internal excitation on the basis of the principle of conservation of energy. The *P*(*E*<sub>T</sub>) has a maximum energy cutoff of 211 ± 21 kJ mol<sup>-1</sup> suggests a reaction energy of -190 ± 21 kJ mol<sup>-1</sup> to form C<sub>5</sub>H<sub>6</sub> isomers along with atomic hydrogen. The distribution maximum of *P*(*E*<sub>T</sub>) is located at 28 ± 3 kJ mol<sup>-1</sup> suggesting a tight exit transition state leading to C<sub>5</sub>H<sub>6</sub> molecules from the C<sub>5</sub>H<sub>7</sub> intermediate(s).<sup>79</sup> An average translational energy of the products calculated to be 59 ± 6 kJ mol<sup>-1</sup> reveals that about 28 ± 3% of the total available energy is deposited into the product translation degrees of freedom. These findings suggest

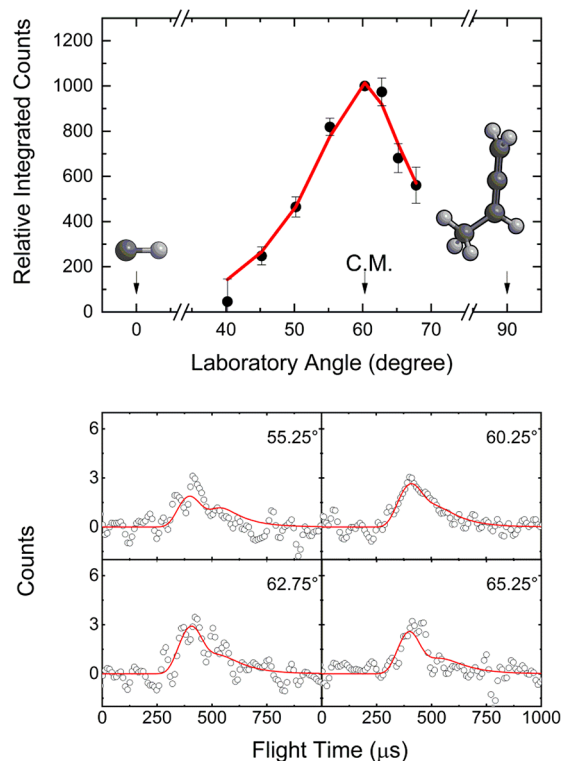


**Figure 1.** Laboratory angular distribution (top) and time-of-flight (TOF) spectra (bottom) recorded at mass-to-charge (*m/z*) 65 (C<sub>5</sub>H<sub>5</sub><sup>+</sup>) from the reaction of the methylidyne radical (CH; C<sub>∞v</sub>; X<sup>2</sup>Π) with 1,2-butadiene (CH<sub>2</sub>CCHCH<sub>3</sub>; C<sub>5</sub>; X<sup>1</sup>A'). The directions of the CH radical and 1,2-butadiene beams are defined as 0° and 90°, respectively. The red solid lines represent the best-fit derived from center-of-mass functions depicted in Figure 2 with black circles defining the experimental data.

indirect reactive scattering dynamics leading to C<sub>5</sub>H<sub>6</sub> isomer(s) via C<sub>5</sub>H<sub>7</sub> intermediate(s).<sup>65,80</sup> Furthermore, the *T*(θ) displays nonzero intensity over the complete angular range from 0° to 180° and is forward-backward symmetric with a maximum at 90° (sideways scattering). This forward-backward symmetry implies that the lifetime of the C<sub>5</sub>H<sub>7</sub> intermediate is longer than its rotational period(s).<sup>81</sup> The sideways scattering suggests significant geometrical constraints on the exit transition state with the hydrogen atom eliminated nearly perpendicular to the rotational plane of the decomposing intermediate and hence almost parallel to the total angular momentum vector.<sup>59,82</sup>

### 4. DISCUSSION

It is always beneficial to merge the experimental results with electronic structure calculations to elucidate the underlying reaction mechanism(s) leading to C<sub>5</sub>H<sub>6</sub> formation (Figures 3–6 and Figures S1–S10; Table 2 and Table S1). The doublet C<sub>5</sub>H<sub>7</sub> potential energy surface (PES) was studied systematically by methylidyne radical (CH) addition to the C–C double bonds of 1,2-butadiene reactant via 79 C<sub>5</sub>H<sub>7</sub> intermediates (i1–i79) and 143 transition states to the hydrogen atom emission products (C<sub>5</sub>H<sub>6</sub>; p1–p17, p20, p21, p25–p30, p36), CH<sub>3</sub> group loss products (C<sub>4</sub>H<sub>4</sub>; p19, p23, p32, p35), C<sub>2</sub>H<sub>3</sub> group loss products (C<sub>3</sub>H<sub>4</sub>; p18, p33), C<sub>3</sub>H<sub>3</sub> group loss product (C<sub>2</sub>H<sub>4</sub>; p24, p31), and C<sub>3</sub>H<sub>5</sub> group loss products (C<sub>2</sub>H<sub>2</sub>; p22, p34, p37) (Figures 3–6 and Figures S1–S5). The intermediates and products that were involved in our previous

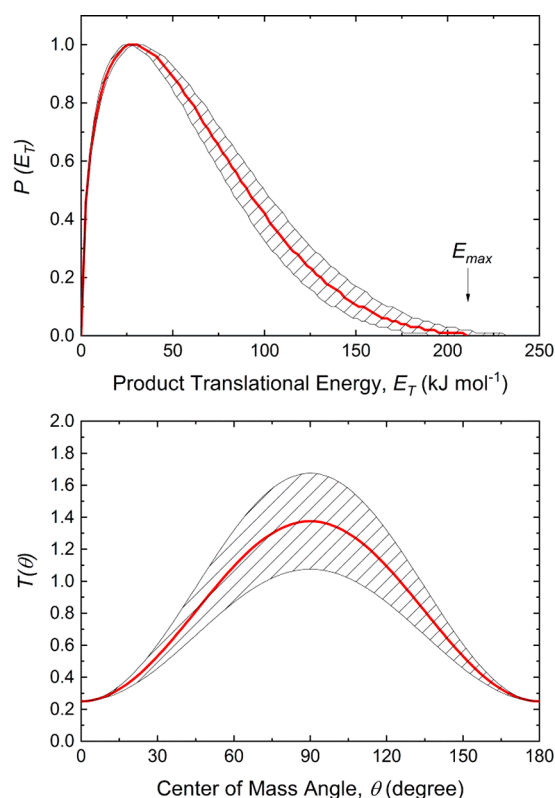


**Figure 2.** Center-of-mass (CM) translational energy  $P(E_T)$  and angular  $T(\theta)$  flux distributions for the CH + 1,2-butadiene reaction. The hatched areas define regions of acceptable fits.

works on methylidyne radical (CH) plus 1,3-butadiene reaction are consistent with the current study.<sup>44</sup> Note that some metastable intermediates are not included in the PES figures. In order to simplify this complicated PES, the latter is divided into six sections:

- (1) Products **p5**, **p14**, **p16**, and **p25–p27** produced by CH radical addition to the terminal and central C=C bonds

of 1,2-butadiene via **i48**, **i49**, **i51**, **i53**, **i55**, **i57**, **i60**, and **i61** (Figure 3).

- (2) Products **p12**, **p13**, and **p17–p22** resulting from the same initial channels involving intermediates **i2**, **i4**, **i7**, **i9**, **i16**, **i17**, **i22–i29**, **i36**, **i39–i43**, **i48**, **i49**, **i51**, **i53**, **i55**, **i57**, **i60**, **i63**, and **i64** (Figures S1–S2).
- (3) Products **p12**, **p17**, and **p28–p30** originating from methylidyne addition to the terminal and central C=C bonds of 1,2-butadiene via **i23**, **i28**, **i29**, **i42**, **i48**, **i50–i53**, **i60**, and **i65–i71** (Figure 4).
- (4) Products **p1–p3**, **p9**, and **p15** produced by CH radical addition to the central C=C bond of 1,2-butadiene through **i3–i6**, **i14**, **i32**, **i51**, **i53**, **i73**, **i75**, and **i79**, (Figure S3).
- (5) Products **p4**, **p6**, **p7**, **p11**, **p16**, **p33**, **p36**, and **p37** stemming from CH radical addition to the central C=C bond of 1,2-butadiene through **i3–i5**, **i10**, **i14**, **i30**, **i37**, **i38**, **i51**, **i53**, **i73**, **i75**, **i77**, and **i79** (Figure S4).
- (6) Products **p22–p24** and **p31–p35** originating from CH radical addition to the terminal and central C=C bonds of 1,2-butadiene through **i8**, **i14**, **i15**, **i31**, **i45**, **i48**, **i49**, **i51**, **i53**, **i55**, **i57**, **i60**, **i63**, **i65–i67**, and **i71** (Figure S5).

Figures S6–S10 trace the hydrogen loss in the methylidyne-1,2-butadiene reaction with hydrogen atom originating from the methylidyne radical; the CH, CH<sub>2</sub>, and CH<sub>3</sub> groups of 1,2-butadiene are highlighted in different colors. Considering the overall reaction energies, cyclopentadiene (**p1**), *trans*-1,2,4-pentatriene (**p2**), *cis*-1,2,4-pentatriene (**p3**), 4-penten-1-yne (**p4**), 1-vinylcyclopropene (**p5**), *cis*-3-vinyl-cyclopropene (**p6**), 4-penten-1-yne (**p7**), 1-penten-3-yne (**p8**), (*Z*)-3-penten-1-yne (**p9**), 1,2,3-pentatriene (**p10**), *trans*-3-vinyl-cyclopropene (**p11**), 1-methyl-1,3-cyclobutadiene (**p12**), 3-methylenecyclobutene (**p13**), cyclopropylacetylene (**p14**), 3-penten-1-yne (**p15**), and 3-ethylidenecyclopropene (**p16**), bicyclo[2.1.0]pent-1(4)-ene (**p17**), 2-methylenebicyclo[1.1.0]butane (**p20**), bicyclo[2.1.0]pent-2-ene (**p21**), spiro[2.2]pent-1-ene (**p25**), 1-vinylcyclopropene (**p26**), ethenylidenecyclopropane (**p27**), 1-methyl-3-methylenecyclopropene (**p28**), 1,2-bis-(methylene)cyclopropane (**p29**), 2-methyl-1-buten-3-yne

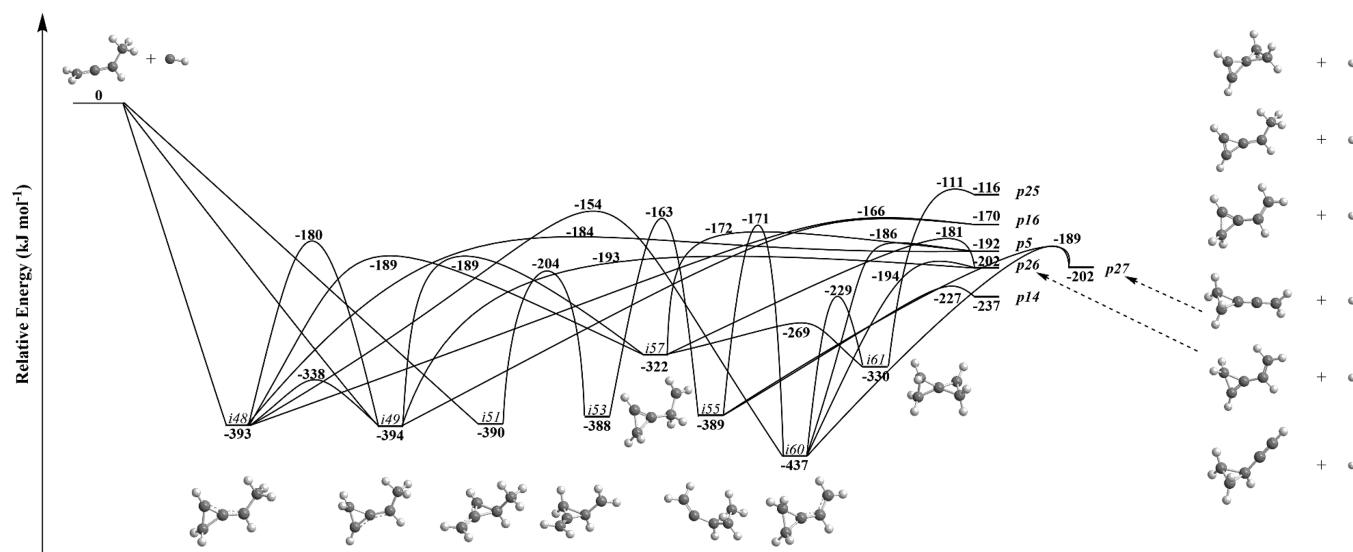


**Figure 3.** Portion of the C<sub>5</sub>H<sub>7</sub> potential energy surface (PES) leading to **p5**, **p14**, **p16**, and **p25–p27** via intermediates **i48**, **i49**, **i51**, **i53**, **i55**, **i57**, **i60**, and **i61**.

Table 2. Statistical Branching Ratios (%) for the Reaction of CH + 1,2-Butadiene at Collision Energy  $E_C$  of 20.6 kJ mol<sup>-1</sup> <sup>a</sup>

product	initial intermediate									
	i46 <sup>b</sup>	i47 <sup>b</sup>	i48 <sup>c</sup>	i49 <sup>c</sup>	i50 <sup>d</sup>	i51 <sup>d</sup>	i8 <sup>e</sup>	i15 <sup>f</sup>	i31 <sup>f</sup>	i65 <sup>g</sup>
total	100	100	100	100	100	100	100	100	100	100
p1	0.7	7.9	0.2	0.2	9.5	9.5	0.5	0.2	0.2	0.0
p2	0.5	6.5	0.1	0.1	7.9	7.9	0.3	0.0	0.0	0.0
p3	0.5	7.1	0.1	0.1	8.5	8.5	13.2	0.1	0.1	0.0
p4	0.1	0.0	0.0	0.0	0.0	0.0	0.0	0.0	0.0	0.4
p5	1.7	0.3	1.8	1.7	0.0	0.0	0.0	0.0	0.0	0.0
p6	0.0	0.0	0.0	0.0	0.0	0.0	0.0	0.0	0.0	0.0
p7	0.1	0.0	0.0	0.0	0.1	0.1	0.0	0.0	0.0	0.5
p8	3.6	0.7	3.8	3.8	0.0	0.0	0.0	7.3	7.3	0.0
p9	2.1	29.2	0.3	0.3	35.2	35.2	1.4	0.1	0.1	0.0
p10	0.1	0.2	0.1	0.1	0.3	0.3	0.0	0.1	0.1	0.0
p11	0.0	0.0	0.0	0.0	0.0	0.0	0.0	0.0	0.0	0.0
p12	0.0	0.0	0.0	0.0	0.0	0.0	0.0	0.0	0.0	0.0
p13	0.0	0.0	0.0	0.0	0.0	0.0	0.0	0.0	0.0	0.1
p14	0.0	0.0	0.0	0.0	0.0	0.0	2.2	0.0	0.0	0.0
p15	2.2	30.6	0.3	0.3	36.9	36.9	1.5	0.1	0.1	0.0
p16	0.8	0.2	0.8	0.8	0.0	0.0	0.0	0.0	0.0	0.0
p17	0.0	0.0	0.0	0.0	0.0	0.0	0.0	0.0	0.0	0.0
p18	0.0	0.0	0.0	0.0	0.0	0.0	0.0	0.0	0.0	0.0
p19	0.0	0.0	0.0	0.0	0.0	0.0	0.0	0.0	0.0	0.0
p20	0.0	0.0	0.0	0.0	0.0	0.0	0.0	0.0	0.0	0.0
p21	0.0	0.0	0.0	0.0	0.0	0.0	0.0	0.0	0.0	0.0
p22	0.0	0.0	0.0	0.0	0.0	0.0	0.0	0.0	0.0	0.0
p23	85.3	15.8	90.6	90.6	0.2	0.2	0.0	92.1	92.1	0.0
p24	0.0	0.4	0.0	0.0	0.5	0.5	80.9	0.0	0.0	0.0
p25	0.0	0.0	0.0	0.0	0.0	0.0	0.0	0.0	0.0	0.0
p26	1.6	0.3	1.7	1.7	0.0	0.0	0.0	0.0	0.0	0.0
p27	0.0	0.0	0.0	0.0	0.0	0.0	0.0	0.0	0.0	0.0
p28	0.0	0.0	0.0	0.0	0.0	0.0	0.0	0.0	0.0	0.3
p29	0.0	0.0	0.0	0.0	0.0	0.0	0.0	0.0	0.0	0.3
p30	0.1	0.0	0.0	0.0	0.0	0.0	0.0	0.0	0.0	50.2
p31	0.1	0.0	0.2	0.2	0.0	0.0	0.0	0.0	0.0	0.0
p32	0.0	0.7	0.0	0.0	0.8	0.8	0.0	0.0	0.0	0.0
p33	0.3	0.1	0.0	0.1	0.1	0.1	0.0	0.0	0.0	1.1
p34	0.1	0.0	0.0	0.0	0.0	0.0	0.0	0.0	0.0	0.4
p35	0.0	0.0	0.0	0.0	0.0	0.0	0.0	0.0	0.0	46.4
p36	0.1	0.0	0.0	0.0	0.0	0.0	0.0	0.0	0.0	0.3
p37	0.0	0.0	0.0	0.0	0.0	0.0	0.0	0.0	0.0	0.0

<sup>a</sup>Here, p1–p37 are cyclopentadiene, *trans*-1,2,4-pentatriene, *cis*-1,2,4-pentatriene, 4-penten-1-yne, 1-vinylcyclopropene, *cis*-3-vinylcyclopropene, 4-penten-1-yne (a conformer of p4), 1-penten-3-yne, (*Z*)-3-penten-1-yne, 1,2,3-pentatriene, *trans*-3-vinyl-cyclopropene, 1-methyl-1,3-cyclobutadiene, 3-methylenecyclobutene, cyclopropylacetylene, (*E*)-3-penten-1-yne, 3-ethylidene-cyclopropene, bicyclo[2.1.0]pent-1(4)-ene, cyclopropane, cyclobutadiene, 2-methylenebicyclo[1.1.0]butane, bicyclo[2.1.0]pent-2-ene, acetylene with *c*-CCH<sub>2</sub>CH<sub>2</sub> radical, 1-buten-3-yne, ethylene with CH<sub>2</sub>CCH radical, spiro[2.2]pent-1-ene, 1-vinyl-cyclopropene (a conformer of p5), ethenylidenecyclopropane, 1-methyl-3-methylenecyclopropene, 1,2-bis(methylene)cyclopropane, 2-methyl-1-buten-3-yne, ethylene with *c*-CCHCH<sub>2</sub> radical, methylenecyclopropane, allene with CHCH<sub>2</sub> radical, acetylene with CH<sub>3</sub>CCH<sub>2</sub> radical, 1,2,3-butatriene, 4-penten-1-yne (a conformer of p4), and acetylene with CH<sub>2</sub>CHCH<sub>2</sub> radical. <sup>b</sup>A metastable intermediate formed by CH addition to the bare C atom in 1,2-butadiene. <sup>c</sup>Formed by CH addition to the terminal C=C bond in 1,2-butadiene. <sup>d</sup>Formed by CH addition to the central C=C bond in 1,2-butadiene. <sup>e</sup>Could be potentially formed by insertion of CH into a C–H in the CH<sub>3</sub> group in 1,2-butadiene. <sup>f</sup>Could be potentially formed by insertion of CH into a C–H in the CH<sub>2</sub> group in 1,2-butadiene. <sup>g</sup>Could be potentially formed by insertion of CH into a C–H in the CH group in 1,2-butadiene.

(p30), and 4-penten-1-yne (p36) isomers can be formed along with the atomic hydrogen with computed reaction energies of –400, –281, –271, –258, –192, –181, –260, –289, –282, –247, –185, –148, –285, –237, –280, –170, –9, –189, –205, –116, –201, –202, –196, –211, –280, and –258 kJ mol<sup>-1</sup>, respectively, with mean errors within 4 kJ mol<sup>-1</sup>. The CH<sub>3</sub>/C<sub>2</sub>H<sub>3</sub>/C<sub>3</sub>H<sub>3</sub>/C<sub>3</sub>H<sub>5</sub> loss products p18, p19, p22, p23, p24, p31, p32, p33, p34, p35, and p37 cannot be detected in the present experiment. The computed reaction energies for the formation of 1-vinylcyclopropene (p5), *cis*-3-vinyl-cyclo-

propene (p6), *trans*-3-vinyl-cyclopropene (p11), 3-ethylidenecyclopropene (p16), methylenebicyclo[1.1.0]butane (p20), bicyclo[2.1.0]pent-2-ene (p21), 1-vinylcyclopropene (p26), ethenylidenecyclopropane (p27), 1-methyl-3-methylenecyclopropene (p28), and 1,2-bis(methylene)cyclopropane (p29) plus atomic hydrogen range between –211 and –170 kJ mol<sup>-1</sup>; these data correlate with our experimentally determined reaction energy of –190 ± 21 kJ mol<sup>-1</sup>. The high-energy isomers—1-methyl-1,3-cyclobutadiene (p12), bicyclo[2.1.0]pent-1(4)-ene (p17), and spiro[2.2]pent-1-ene (p25)—might

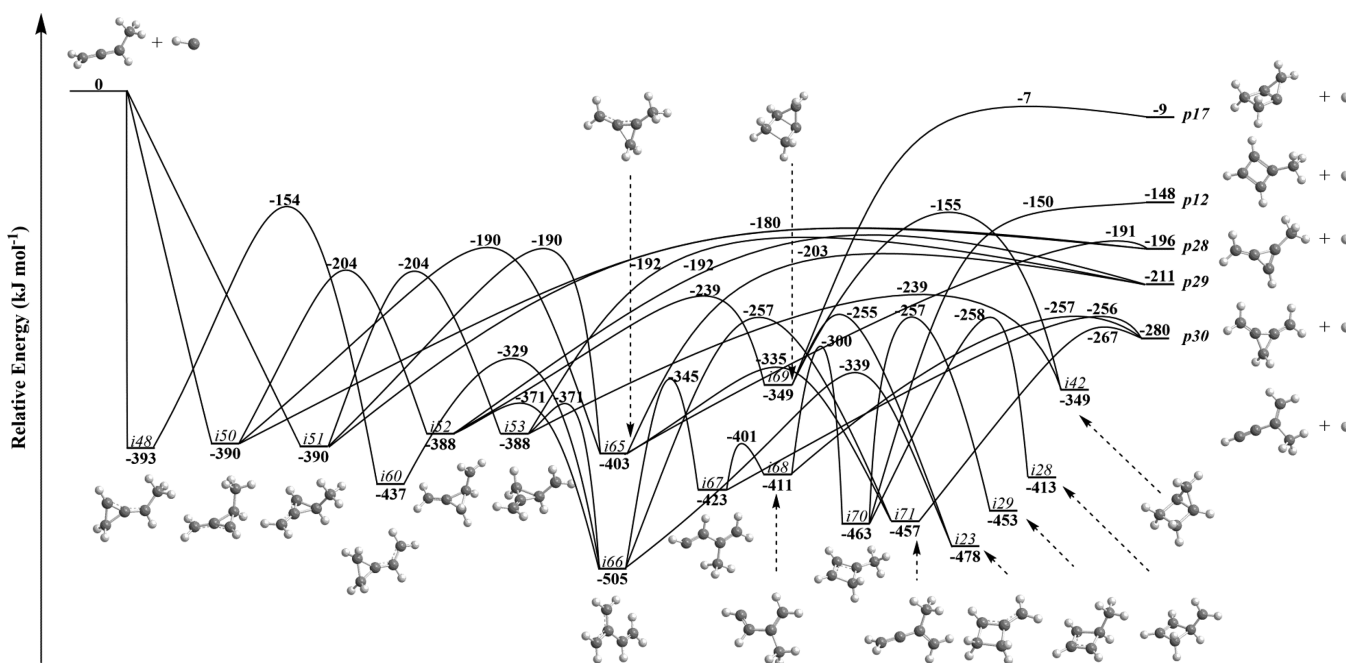


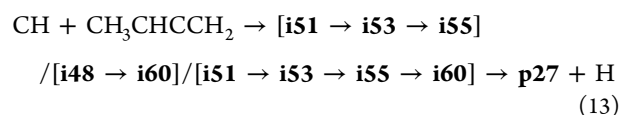
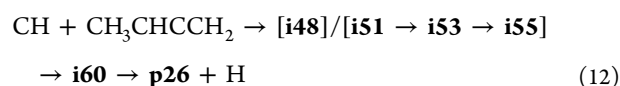
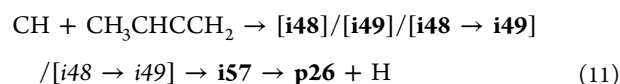
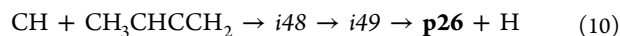
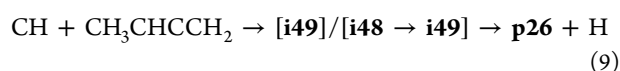
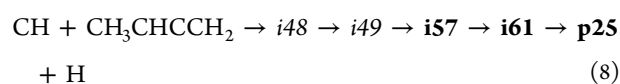
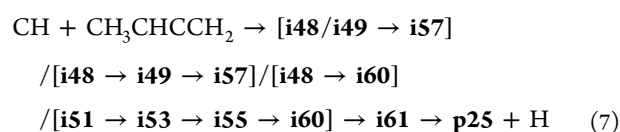
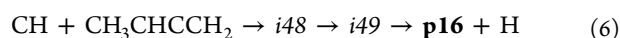
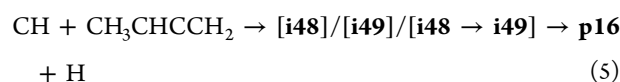
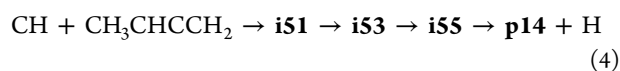
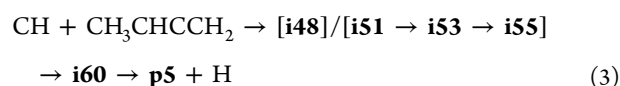
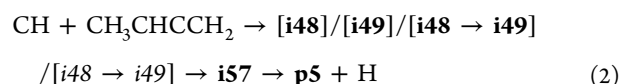
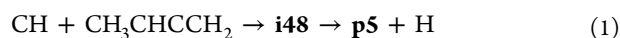
Figure 4. Portion of  $C_5H_7$  PES leading to **p12**, **p17**, and **p28–p30** via intermediates **i23**, **i28**, **i29**, **i42**, **i48**, **i50–i53**, **i60**, and **i65–i71**.

be masked in the low energy portion of the  $P(E_T)$ . However, if solely formed, the  $P(E_T)$  values for **p12**, **p17**, and **p25** would have a maximum energy cutoff of 169, 30, and 137  $\text{kJ mol}^{-1}$ , respectively, leading to relatively narrow LAD and TOF spectra. In order to better correlate the experimental and theoretical results, we focus on the discussion of pathways (Figures 3 and 4) that lead to the products potentially observed in experiment. The details of the other reaction pathways (Figures S1–S5) may be found in Supporting Information.

**4.1. The CH Radical Addition to the Terminal and Central C=C Bonds of 1,2-Butadiene Resulting in Products p5, p14, p16, and p25–p27 via Intermediates i48, i49, i51, i53, i55, i57, i60, and i61 (Figure 3).** The CH radical can add barrierlessly to the terminal and central C=C bonds of 1,2-butadiene forming the initial three-member adducts **i48/i49** and **i51**, respectively. Two conformers of the 1-vinylcyclopropene product (**p5** and **p26**) can be formed via hydrogen atom emission from the  $\text{CH}_3$  group in **i48** and **i49**, respectively, via loose exit transition states lying close to 8  $\text{kJ mol}^{-1}$  above the separated products. The  $\text{CHCH}_3$  moiety rotation in **i48** leads to **i49** via a moderate barrier of 55  $\text{kJ mol}^{-1}$  above **i48**. Intermediate **i49** is also connected with **i48** via a high barrier of 213  $\text{kJ mol}^{-1}$  above **i48** as H shift from the  $\text{CH}_2$  moiety to the adjacent CH group in **i48**; the decomposition of both isomers leads to the 3-ethylidenecyclopropene (**p16**) product via atomic hydrogen loss from the  $\text{CH}_2$  group in **i48** and **i49**. A hydrogen atom migration from the terminal  $\text{CH}_3$  group to the adjacent CH moiety of **i48** and **i49** results in intermediate **i57**. Two different conformers of 1-vinylcyclopropene (**p5** and **p26**) can also be formed via hydrogen atom emission from the nonterminal  $\text{CH}_2$  moiety in **i57** via tight exit transition states lying close to 20  $\text{kJ mol}^{-1}$  above the separated products. A 1,4-H migration from the  $\text{CH}_3$  moiety to the CH group in the three-member ring of **i48** leads to intermediate **i60**; a similar 1,3-hydrogen atom shift also interconverts intermediates **i51** and **i53**. The ring opening and the ring reformation by creation of a C–C bond between the

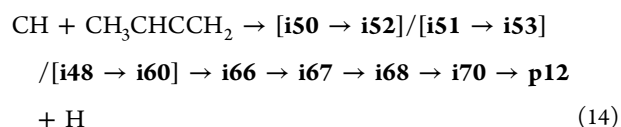
$\text{CH}_2$  groups of **i53** (“methylene walk”) results in the three-member cyclic intermediate **i55** accessed via a barrier of 225  $\text{kJ mol}^{-1}$  above **i53**; the decomposition of **i55** yields cyclopropylacetylene (**p14**) via atomic hydrogen loss from the terminal  $\text{CH}_2$  group of **i55**. The intermediate **i60** can also be generated via a hydrogen migration from the CH group to the adjacent bare carbon moiety in **i55**. Both isomers can eliminate a hydrogen atom from the CH moiety leading to the product ethenylidenecyclopropane (**p27**). The 1-vinylcyclopropene products (**p5** and **p26**) can be produced via atomic hydrogen emission from the  $c\text{-CCH}_2\text{CH}_2$  moiety of **i60** via loose exit transition states lying 6 and 8  $\text{kJ mol}^{-1}$  above the separated products, respectively. The second three-member ring closures in **i57** and **i60** lead to a bicyclic spiran-like intermediate **i61**; the decomposition of the latter yields spiro[2.2]pent-1-ene (**p25**) via hydrogen atom loss from the  $\text{CH}_2$  moiety of the  $c\text{-CCHCH}_2$  group in **i61**. In brief, **p5** can be formed via pathways 1 and 2 with a hydrogen loss from the 1,2-butadiene reactant and via pathway 3 with hydrogen emission possible from both reactants. Since there are two transition states between **i48** and **i49**, we use **i48**  $\rightarrow$  **i49** and **i48**  $\rightarrow$  **i49** to denote the conformational change and hydrogen migration processes, respectively. Product **p14** and **p27** can be accessed via pathways 4 and 13, respectively, with the hydrogen atom loss originating from the  $\text{CH}_2$  group of the 1,2-butadiene reactant. Product **p16** is produced via pathway 5 with the atomic hydrogen emission from the  $\text{CH}_2$  group of 1,2-butadiene and via pathway 6 with hydrogen atom loss both from the methylidyne radical reactant and the  $\text{CH}_2$  group of 1,2-butadiene. Product **p25** may be formed through pathway 7 with the hydrogen loss from 1,2-butadiene and via pathway 8 with atomic hydrogen emission from both the radical reactant and the  $\text{CH}_2$  group of 1,2-butadiene. Product **p26** is reached via pathways 9–11 with H atom loss from the 1,2-butadiene reactant and via pathway 12 with the hydrogen loss from both reactants. Considering the experimentally derived reaction energy of  $-190 \pm 21 \text{ kJ mol}^{-1}$ , the products 1-vinylcyclopropene (**p5** and **p26**), 3-ethylidenecyclopropene

(p16), and ethenylidenecyclopropane (p27) with reaction energies of  $-192$ ,  $-202$ ,  $-170$ , and  $-202$   $\text{kJ mol}^{-1}$ , respectively, are the most likely reaction products. Considering significant barriers of over  $200$   $\text{kJ mol}^{-1}$ , the hydrogen shifts between i48 to i49, i48/i49 to i57, i48 to i60, i53 to i55, and i55 to i60 are less competitive than the conformational change i48  $\rightarrow$  i49; hence, we may rule out the pathways 2–3, 6–8, 10–12, and 13 leading to p5, p16, p25, p26, and p27. Therefore, p5, p16, and p26 can likely be formed under our experimental conditions via pathways 1, 5, and 9, respectively.



**4.2. The CH Radical Addition to the Terminal and Central C=C bonds of 1,2-Butadiene Leading to Products p12, p17, and p28–p30 via i23, i28, i29, i42, i48, i50–i53, i60, and i65–i71 (Figure 4).** The barrierless addition of the CH radical to the central C=C bond of 1,2-butadiene leads to adducts i50 and i51. 1-Methyl-3-methylenecyclopropene (p28) can be formed via atomic hydrogen emission from the CH moiety of the CHCH<sub>3</sub> group in i50 and i51 via a tight exit transition state lying  $16$   $\text{kJ mol}^{-1}$  above the separated products. A hydrogen atom migration from the CH<sub>3</sub> group to the nonadjacent CH group in i50 leads

to intermediate i52 via a barrier of  $186$   $\text{kJ mol}^{-1}$  above i50. The intermediate i65 can be accessed via H migration between CH moieties in i50 and i51. The product 1,2-bis(methylene)cyclopropane (p29) can be formed via H atom loss from the CH<sub>3</sub> group of i65 via a loose exit transition state lying  $8$   $\text{kJ mol}^{-1}$  above the separated products. Alternatively, a ring opening of intermediates i52, i53, and i60 leads to the acyclic intermediate i66; the decomposition of i52 and/or i53 yields 1,2-bis(methylene)cyclopropane (p29) via atomic hydrogen emission from the CH moiety of i52 and/or i53. The C–C bond formation between two terminal CH<sub>2</sub> moieties in i52 forms a four-member ring and produces a bicyclic intermediate i69. The product bicyclo[2.1.0]pent-1(4)-ene (p17) can be formed via H atom elimination from the CH group of i69 via a loose exit transition state lying  $2$   $\text{kJ mol}^{-1}$  above the separated products. A hydrogen migration from the CH<sub>2</sub> group of terminal CHCH<sub>2</sub> moiety to one of the terminal CH<sub>2</sub> groups in i66 leads to i67, while the ring opening of i65 and a 1,3-hydrogen shift from CH moiety to the nonadjacent CH<sub>2</sub> group in i66 both lead to i71. The product 2-methyl-1-buten-3-yne (p30) can be formed via H atom emission from the terminal CH<sub>2</sub>C moiety of i71 via a loose exit transition state lying  $13$   $\text{kJ mol}^{-1}$  above the separated products. The conformers i67 and i68 are connected via a low barrier of  $22$   $\text{kJ mol}^{-1}$  above i67; the product 2-methyl-1-buten-3-yne (p30) can be accessed via H atom loss from the nonterminal CH moiety of both intermediates via tight exit transition states lying  $24$  and  $23$   $\text{kJ mol}^{-1}$  above the separated products, respectively. The C–C bond formation between the terminal CH and CH<sub>2</sub> moieties of i68 lead to a four-member cyclic intermediate i70 and the decomposition of i70 yields the product 1-methyl-1,3-cyclobutadiene (p12) via atomic hydrogen emission from the CH<sub>2</sub> moiety of i70. Here, similar to i29–p19, the transition state for i70–p12 could be found at the DFT level, but its energy sinks below the product at CCSD(T)-F12 indicating that the reverse hydrogen atom addition to methylcyclobutadiene most likely occurs without barrier. In brief, p12 can be formed via pathway 14 with H atom emission from the CH<sub>2</sub> moiety of 1,2-butadiene or from both CH radical and the CH<sub>3</sub> group of 1,2-butadiene. The products p17 and p28 can be accessed through pathways 15 and 16, respectively, with hydrogen loss from the CH group of 1,2-butadiene. The product p29 can be produced via pathways 17 and 18 with the H atom emission from the methylidyne radical reactant or the CH<sub>3</sub> group of 1,2-butadiene. The product p30 can be formed via pathway 19 with hydrogen emission from the CH group of 1,2-butadiene; this product can be also reached via pathways 20 and 21 with hydrogen atom loss from the CH<sub>3</sub> and the CH<sub>2</sub> groups of 1,2-butadiene. Considering the experimentally derived reaction energy of  $-190 \pm 21$   $\text{kJ mol}^{-1}$ , the 1-methyl-3-methylenecyclopropene (p28) and 1,2-bis(methylene)cyclopropane (p29) with the reaction energies of  $-196$  and  $-211$   $\text{kJ mol}^{-1}$  are among likely reaction products. Due to high barriers of  $200$   $\text{kJ mol}^{-1}$ , the isomerization processes from i50 to i65 and from i51 to i65, are expected to be somewhat less competitive than i50  $\rightarrow$  i52 and i51  $\rightarrow$  i53, respectively. Therefore, p28 and p29 can be more likely formed via pathways 16 and 18, respectively.



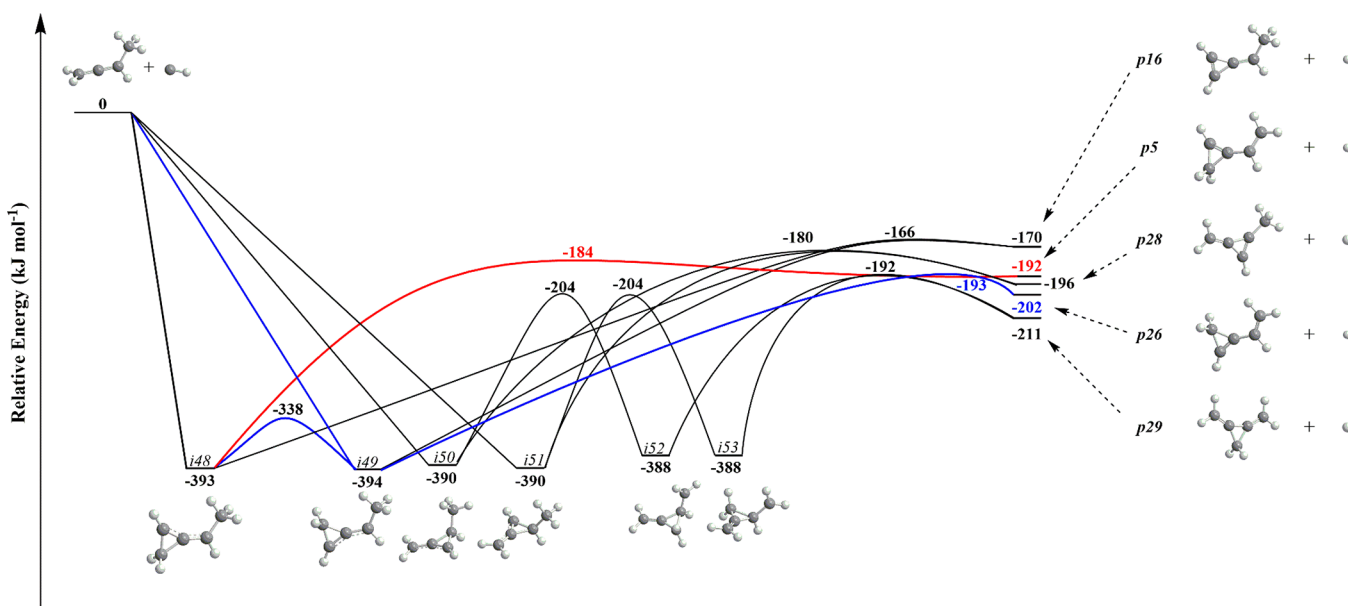


Figure 5. Reduced  $C_5H_7$  PES leading to **p5**, **p16**, **p26**, **p28**, and **p29**. Pathways leading to **p5** and **p26** are colored in red and blue, respectively.

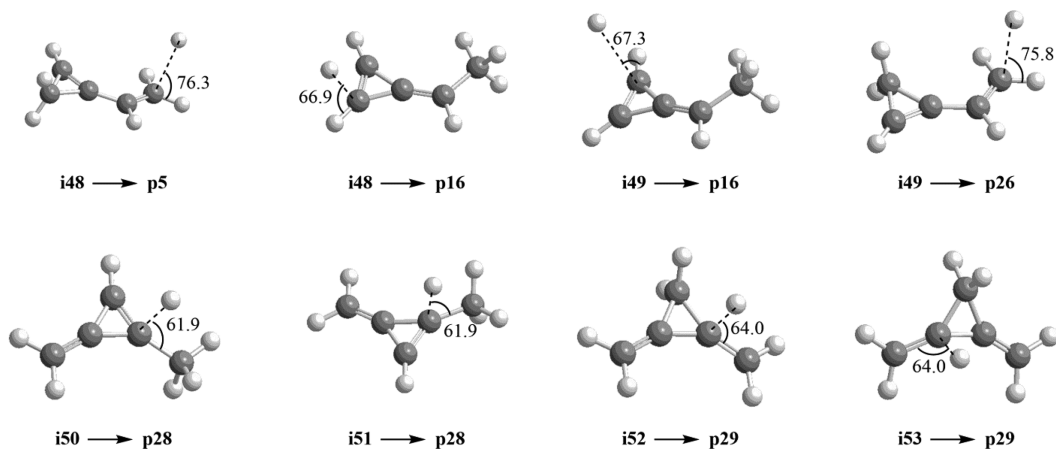
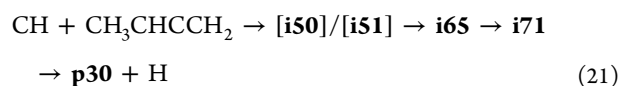
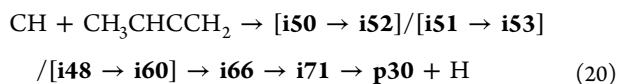
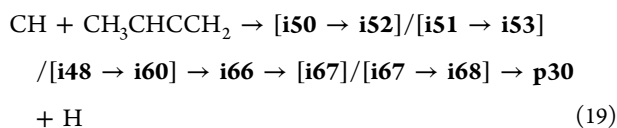
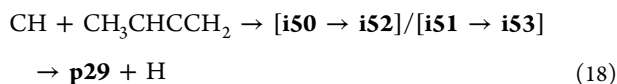
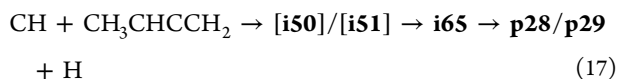
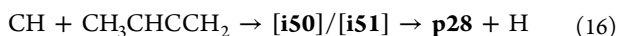
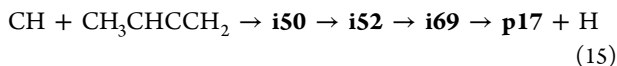


Figure 6. Computed geometries of the exit transition states leading to **p5**, **p16**, **p26**, **p28**, and **p29**. Angles of the departing hydrogen atoms are given in degrees with respect to the rotation plane of the decomposing complex.



In summary, considering the experimentally derived reaction energy of  $-190 \pm 21$  kJ mol<sup>-1</sup>, together with elimination of isomerization processes with high barriers of over 200 kJ mol<sup>-1</sup>, 1-vinyl-cyclopropene conformers (**p5** and **p26**), 3-ethylidenecyclopropene (**p16**), 1-methyl-3-methylenecyclopropene (**p28**), and 1,2-bis(methylene)cyclopropane (**p29**) along with atomic hydrogen are likely formed under our experimental conditions (Figure 5). The product **p5** can be formed via pathway 1; **p16** may be reached via pathway 5; **p26** can be accessed through pathway 9; **p28** may be formed via pathway 16, whereas **p29** can be generated through pathway 18. Note that the pathways 1, 5, and 9 leading to **p5**, **p16**, and **p26** are accessed via the barrierless addition of the CH radical to the terminal C=C bond of 1,2-butadiene, whereas pathways 16 and 18 generating **p28** and **p29** are reached via a barrierless addition of the methylidyne radical to the central C=C bond. Recall that the best fit center-of-mass angular

distribution peaked at 90° (sideways scattering) suggesting that the dominating decomposition pathway of the C<sub>5</sub>H<sub>7</sub> intermediate involves a hydrogen atom which is ejected perpendicularly to the rotational plane of the decomposing complex. The computed geometries of the exit transition states lead to **p5**, **p16**, **p26**, **p28** and **p29** connecting the intermediates to these products via pathways 1, 5, 9, 16, and 18 can account for the sideways scattering (Figure 6). Among them, the transition states for **i48** → **p5** and **i49** → **p26** with the hydrogen atom ejected at angles of 76.3° and 75.8°, which are closest to 90°, suggest that **p5** and **p26** are the most likely products formed under our experimental conditions via pathways 1 and 9, respectively, with the hydrogen atom emission from the methyl group of 1,2-butadiene. Note that our data suggest a rather tight exit transition state leading to C<sub>5</sub>H<sub>6</sub> isomer(s). This can be accounted for with the formation of **p26**, **p28**, and **p29**. Consequently, pathways leading to **p5** and **p26** fulfill the requirement of a tight exit transition state, a hydrogen loss perpendicular to the rotation plane of the decomposing complex, and the experimentally derived reaction energy. However, considering the low frequency bending modes of the C–H bond involved in the decomposing intermediate leading to **p28** and **p29**, these products cannot be entirely dismissed since these vibrations could average out to a hydrogen loss perpendicular to the rotation plane of the decomposing complex.

Finally, we explored the yields of the individual products **p1**–**p37** using statistical RRKM theory (Table 2) at  $E_c = 20.6$  kJ mol<sup>-1</sup> within the zero-pressure limit. RRKM predicts, in the case of the methylidyne radical addition to the terminal C=C double bond of 1,2-butadiene, vinylacetylene (**p23**) along with the methyl radical to be the most likely product (90.6%) (see Figure S5), whereas 1-vinylcyclopropenes (**p5** and **p26**), 1-penten-3-yne (**p8**), and 3-ethylidenecyclopropene (**p16**) are minor products (<4% each); (*Z*)-3-penten-1-yne (**p9**, 35.2%) and (*E*)-3-penten-1-yne (**p15**, 36.9%) are the main products via methylidyne radical addition to the central C–C double bond of 1,2-butadiene along with cyclopentadiene (**p1**), *trans*-1,2,4-pentatriene (**p2**) and *cis*-1,2,4-pentatriene (**p3**) being minor products (<10% each). Entrance channels involving methylidyne insertions into various C–H bonds in 1,2-butadiene may result in somewhat different statistical product distributions (Table 2) but those are expected to be much less likely than methylidyne addition to the C=C double bonds. The significant difference between our experimental results under single-collision conditions and RRKM calculations indicates a non-RRKM behavior of this bimolecular reaction yielding at least two conformers of 1-vinylcyclopropene (**p5** and **p26**) with a lifetime of the initial addition adducts **i48**/**i49** not long enough to allow energy randomization to occur. A similar behavior was also revealed in the bimolecular reactions of the CH radical with 1,3-butadiene.<sup>40</sup> Here, the CH radical added barrierlessly to the C=C bond of 1,3-butadiene eventually leading to the cyclic *cis*- and *trans*-3-vinyl-cyclopropene conformers ( $\Delta_r G = -119$  kJ mol<sup>-1</sup>) with H loss from the terminal CH<sub>2</sub> group of the 1,3-butadiene reactant via exit transition states lying 5–33 kJ mol<sup>-1</sup> above the separated products. Thus, for both reactions, a dynamically preferable scenario of methylidyne addition to a double C=C followed by immediate hydrogen atom loss is fulfilled rather than the statistically favored (multistep) isomerization followed by fragmentation.

## 5. CONCLUSION

The crossed molecular beam reactions of the methylidyne radical (CH; X<sup>2</sup>Π) with 1,2-butadiene (CH<sub>2</sub>CCHCH<sub>3</sub>; X<sup>1</sup>A') were studied at collision energies of about 21 kJ mol<sup>-1</sup>. Combining our experimental data with the doublet C<sub>5</sub>H<sub>7</sub> PES, the CH radical may add barrierlessly to the carbon–carbon double bonds of 1,2-butadiene yielding cyclic doublet C<sub>5</sub>H<sub>7</sub> intermediates; these collision complexes are suggested to undergo nonstatistical, unimolecular decomposition via hydrogen atom loss from the 1,2-butadiene reactant yielding the cyclic 1-vinyl-cyclopropene conformers (**p5** and **p26**;  $\Delta_r G = -192$  and  $-202$  kJ mol<sup>-1</sup>, respectively), 1-methyl-3-methylenecyclopropene (**p28**;  $\Delta_r G = -196$  kJ mol<sup>-1</sup>), and/or 1,2-bis(methylene)cyclopropane (**p29**;  $\Delta_r G = -211$  kJ mol<sup>-1</sup>); the overall reaction exoergicity was determined to be  $-190 \pm 21$  kJ mol<sup>-1</sup>. The CH radical addition to the terminal carbon–carbon double bond of 1,2-butadiene leads to three-member cyclic C<sub>5</sub>H<sub>7</sub> intermediates **i48**, and/or **i49**. The decomposition of both intermediates results in 1-vinylcyclopropene conformers (**p5** and **p26**;  $\Delta_r G = -192$  and  $-202$  kJ mol<sup>-1</sup>, respectively) via hydrogen atom emission from the CH<sub>3</sub> group. The CH radical addition to the central C=C bond of 1,2-butadiene generates three-member cyclic C<sub>5</sub>H<sub>7</sub> intermediates **i50**, and/or **i51**; the decomposition of intermediates **i50** and/or **i51** produces 1-methyl-3-methylenecyclopropene (**p28**;  $\Delta_r G = -196$  kJ mol<sup>-1</sup>) via H loss from the CH group of the 1,2-butadiene reactant via a tight exit transition state. A hydrogen atom shift from the methyl group to the nonadjacent methylidyne group in **i50** and **i51** may lead to the intermediates **i52** and **i53**, respectively; the decomposition of **i52** and/or **i53** yields 1,2-bis(methylene)cyclopropane (**p29**;  $\Delta_r G = -211$  kJ mol<sup>-1</sup>) via atomic hydrogen emission from the CH moiety of 1,2-butadiene reactant. Considering the barrierless nature of the reaction, these cyclic C<sub>5</sub>H<sub>6</sub> molecule can be synthesized even in cold regions of the interstellar medium such as the Taurus Molecular Cloud (TMC-1). Furthermore, in high-temperature settings such as combustion flames and circumstellar envelopes of carbon stars, cyclic C<sub>5</sub>H<sub>6</sub> isomers with a three-member ring might easily undergo hydrogen-assisted isomerization to the cyclopentadiene (*c*-C<sub>5</sub>H<sub>6</sub>), followed by hydrogen abstraction/loss and ultimately yielding the cyclopentadienyl radical (*c*-C<sub>5</sub>H<sub>5</sub>), which is believed to be a key precursor to PAHs and carbonaceous nanoparticles.<sup>33,83</sup>

## ■ ASSOCIATED CONTENT

### Supporting Information

The Supporting Information is available free of charge at <https://pubs.acs.org/doi/10.1021/acs.jpca.0c08731>.

Discussion of the formation pathways of products **p12**, **p13**, and **p17**–**p22** (Figures S1 and S2), products **p1**–**p3**, **p9**, and **p15** (Figure S3), products **p4**, **p6**, **p7**, **p11**, **p16**, **p33**, **p36**, and **p37** (Figure S4), and products **p22**–**p24** and **p31**–**p35** (Figure S5), rate constants (Table S1), and optimized Cartesian coordinates and calculated vibrational frequencies of the reactants, products, intermediates, and transition states (PDF)

## ■ AUTHOR INFORMATION

### Corresponding Authors

Ralf I. Kaiser – Department of Chemistry, University of Hawaii'i at Manoa, Honolulu, Hawaii 96822, United States;

orcid.org/0000-0002-7233-7206; Email: ralfk@hawaii.edu

Alexander M. Mebel – Department of Chemistry and Biochemistry, Florida International University, Miami, Florida 33199, United States; orcid.org/0000-0002-7233-3133; Email: mebela@fiu.edu

## Authors

Chao He – Department of Chemistry, University of Hawai'i at Manoa, Honolulu, Hawaii 96822, United States

Anatoliy A. Nikolayev – Samara National Research University, Samara 443086, Russian Federation

Long Zhao – Department of Chemistry, University of Hawai'i at Manoa, Honolulu, Hawaii 96822, United States

Aaron M. Thomas – Department of Chemistry, University of Hawai'i at Manoa, Honolulu, Hawaii 96822, United States;

orcid.org/0000-0001-8540-9523

Srinivas Doddipatla – Department of Chemistry, University of Hawai'i at Manoa, Honolulu, Hawaii 96822, United States

Galiya R. Galimova – Samara National Research University, Samara 443086, Russian Federation; Department of Chemistry and Biochemistry, Florida International University, Miami, Florida 33199, United States

Valeriy N. Azyazov – Samara National Research University, Samara 443086, Russian Federation; Lebedev Physical Institute, Samara 443011, Russian Federation

Complete contact information is available at:

<https://pubs.acs.org/10.1021/acs.jpca.0c08731>

## Author Contributions

<sup>†</sup>C.H. and A.A.N. contributed equally to this work.

## Notes

The authors declare no competing financial interest.

## ACKNOWLEDGMENTS

This work was supported by the U.S. Department of Energy, Basic Energy Sciences Grants DE-FG02-03ER15411 and DE-FG02-04ER15570 to the University of Hawaii and to Florida International University, respectively. Ab initio calculations at Samara University were supported by the Ministry of Science and Higher Education of the Russian Federation under Grant No. 14.Y26.31.0020.

## REFERENCES

- (1) Gredel, R. Interstellar C<sub>2</sub> Absorption Lines Towards CH<sup>+</sup> Forming Regions. *Astron. Astrophys.* **1999**, 351, 657–668.
- (2) Tielens, A. G. G. M. Interstellar Polycyclic Aromatic Hydrocarbon Molecules. *Annu. Rev. Astron. Astrophys.* **2008**, 46, 289–337.
- (3) Ehrenfreund, P.; Sephton, M. A. Carbon Molecules in Space: from Astrochemistry to Astrobiology. *Faraday Discuss.* **2006**, 133, 277–288.
- (4) Eaves, N. A.; Dworkin, S. B.; Thomson, M. J. Assessing Relative Contributions of PAHs to Soot Mass by Reversible Heterogeneous Nucleation and Condensation. *Proc. Combust. Inst.* **2017**, 36, 935–945.
- (5) Jones, B. M.; Zhang, F.; Kaiser, R. I.; Jamal, A.; Mebel, A. M.; Cordiner, M. A.; Charnley, S. B. Formation of Benzene in the Interstellar Medium. *Proc. Natl. Acad. Sci. U. S. A.* **2011**, 108, 452–457.
- (6) Mebel, A. M.; Landera, A.; Kaiser, R. I. Formation Mechanisms of Naphthalene and Indene: From the Interstellar Medium to Combustion Flames. *J. Phys. Chem. A* **2017**, 121, 901–926.
- (7) Kaiser, R. I.; Parker, D. S. N.; Mebel, A. M. Reaction Dynamics in Astrochemistry: Low-Temperature Pathways to Polycyclic

Aromatic Hydrocarbons in the Interstellar Medium. *Annu. Rev. Phys. Chem.* **2015**, 66, 43–67.

(8) Steglich, M.; Bouwman, J.; Huisken, F.; Henning, T. Can Neutral and Ionized Polycyclic Aromatic Hydrocarbons be Carriers of the Ultraviolet Extinction Bump and the Diffuse Interstellar Bands? *Astrophys. J.* **2011**, 742, 2–12.

(9) Zenobi, R.; Philippoz, J.-M.; Zare, R. N.; Wing, M. R.; Bada, J. L.; Marti, K. Organic Compounds in the Forest Vale, H4 Ordinary Chondrite. *Geochim. Cosmochim. Acta* **1992**, 56, 2899–2905.

(10) Busby, W. F., Jr; Stevens, E. K.; Kellenbach, E. R.; Cornelisse, J.; Lugtenburg, J. Dose-Response Relationships of the Tumorigenicity of Cyclopenta[cd]pyrene, Benzo[a]pyrene and 6-Nitrochrysene in a Newborn Mouse Lung Adenoma Bioassay. *Carcinogenesis* **1988**, 9, 741–746.

(11) Kim, K.-H.; Jahan, S. A.; Kabir, E.; Brown, R. J. C. A Review of Airborne Polycyclic Aromatic Hydrocarbons (PAHs) and Their Human Health Effects. *Environ. Int.* **2013**, 60, 71–80.

(12) Durant, J. L.; Busby, W. F., Jr; Lafleur, A. L.; Penman, B. W.; Crespi, C. L. Human Cell Mutagenicity of Oxygenated, Nitrated and Unsubstituted Polycyclic Aromatic Hydrocarbons Associated with Urban Aerosols. *Mutat. Res., Genet. Toxicol. Test.* **1996**, 371, 123–157.

(13) Zhao, L.; Kaiser, R. I.; Xu, B.; Ablikim, U.; Ahmed, M.; Evseev, M. M.; Bashkurov, E. K.; Azyazov, V. N.; Mebel, A. M. Low-Temperature Formation of Polycyclic Aromatic Hydrocarbons in Titan's Atmosphere. *Nat. Astron.* **2018**, 2, 973–979.

(14) Tielens, A. G. G. M. The Molecular Universe. *Rev. Mod. Phys.* **2013**, 85, 1021–1081.

(15) Gilmour, I.; Pillinger, C. T. Isotopic Compositions of Individual Polycyclic Aromatic Hydrocarbons from the Murchison Meteorite. *Mon. Not. R. Astron. Soc.* **1994**, 269, 235–240.

(16) Naraoka, H.; Shimoyama, A.; Harada, K. Isotopic Evidence from an Antarctic Carbonaceous Chondrite for Two Reaction Pathways of Extraterrestrial PAH Formation. *Earth Planet. Sci. Lett.* **2000**, 184, 1–7.

(17) Zhang, F.; Gu, X.; Guo, Y.; Kaiser, R. I. Reaction Dynamics on the Formation of Styrene: A Crossed Molecular Beam Study of the Reaction of Phenyl Radicals with Ethylene. *J. Org. Chem.* **2007**, 72, 7597–7604.

(18) Landera, A.; Kaiser, R. I.; Mebel, A. M. Addition of One and Two Units of C<sub>2</sub>H to Styrene: A Theoretical Study of the C<sub>10</sub>H<sub>9</sub> and C<sub>12</sub>H<sub>9</sub> Systems and Implications Toward Growth of Polycyclic Aromatic Hydrocarbons at Low Temperatures. *J. Chem. Phys.* **2011**, 134, 024302.

(19) Zhao, L.; Kaiser, R. I.; Lu, W.; Ahmed, M.; Evseev, M. M.; Bashkurov, E. K.; Azyazov, V. N.; Tönshoff, C.; Reicherter, F.; Bettinger, H. F.; et al. A Free-Radical Prompted Barrierless Gas-Phase Synthesis of Pentacene. *Angew. Chem., Int. Ed.* **2020**, 59, 11334–11338.

(20) He, C.; Thomas, A. M.; Galimova, G. R.; Morozov, A. N.; Mebel, A. M.; Kaiser, R. I. Gas-Phase Formation of Fulvenallene (C<sub>7</sub>H<sub>6</sub>) via the Jahn-Teller Distorted Tropyl (C<sub>7</sub>H<sub>7</sub>) Radical Intermediate under Single-Collision Conditions. *J. Am. Chem. Soc.* **2020**, 142, 3205–3213.

(21) Thomas, A. M.; Doddipatla, S.; Kaiser, R. I.; Galimova, G. R.; Mebel, A. M. A Barrierless Pathway Accessing the C<sub>9</sub>H<sub>9</sub> and C<sub>9</sub>H<sub>8</sub> Potential Energy Surfaces via the Elementary Reaction of Benzene with 1-Propynyl. *Sci. Rep.* **2019**, 9, 17595.

(22) Lucas, M.; Thomas, A. M.; Zhao, L.; Kaiser, R. I.; Kim, G. S.; Mebel, A. M. Gas-Phase Synthesis of the Elusive Cyclooctatetraenyl Radical (C<sub>8</sub>H<sub>7</sub>) via Triplet Aromatic Cyclooctatetraene (C<sub>8</sub>H<sub>8</sub>) and Non-Aromatic Cyclooctatriene (C<sub>8</sub>H<sub>8</sub>) Intermediates. *Angew. Chem., Int. Ed.* **2017**, 56, 13655–13660.

(23) Yang, T.; Kaiser, R. I.; Troy, T. P.; Xu, B.; Kostko, O.; Ahmed, M.; Mebel, A. M.; Zagidullin, M. V.; Azyazov, V. N. HACA's Heritage: A Free-Radical Pathway to Phenanthrene in Circumstellar Envelopes of Asymptotic Giant Branch Stars. *Angew. Chem., Int. Ed.* **2017**, 56, 4515–4519.

- (24) Baroncelli, M.; Mao, Q.; Galle, S.; Hansen, N.; Pitsch, H. Role of Ring-Enlargement Reactions in the Formation of Aromatic Hydrocarbons. *Phys. Chem. Chem. Phys.* **2020**, *22*, 4699–4714.
- (25) McEnally, C. S.; Pfeifferle, L. D.; Atakan, B.; Kohse-Höinghaus, K. Studies of Aromatic Hydrocarbon Formation Mechanisms in Flames: Progress towards Closing the Fuel Gap. *Prog. Energy Combust. Sci.* **2006**, *32*, 247–294.
- (26) Johansson, K. O.; Head-Gordon, M. P.; Schrader, P. E.; Wilson, K. R.; Michelsen, H. A. Resonance-Stabilized Hydrocarbon-Radical Chain Reactions may Explain Soot Inception and Growth. *Science* **2018**, *361*, 997–1000.
- (27) Melius, C. F.; Colvin, M. E.; Marinov, N. M.; Pit, W. J.; Senkan, S. M. Reaction Mechanisms in Aromatic Hydrocarbon Formation involving the C<sub>5</sub>H<sub>3</sub> Cyclopentadienyl Moiety. *Symp. (Int.) Combust., [Proc.]* **1996**, *26*, 685–692.
- (28) Moskaleva, L. V.; Mebel, A. M.; Lin, M. C. The CH<sub>3</sub> + C<sub>5</sub>H<sub>5</sub> Reaction: A Potential Source of Benene at High Temperatures. *Symp. (Int.) Combust., [Proc.]* **1996**, *26*, 521–526.
- (29) Fascella, S.; Cavallotti, C.; Rota, R.; Carrà, S. The Peculiar Kinetics of the Reaction between Acetylene and the Cyclopentadienyl Radical. *J. Phys. Chem. A* **2005**, *109*, 7546–7557.
- (30) Savee, J. D.; Selby, T. M.; Welz, O.; Taatjes, C. A.; Osborn, D. L. Time- and Isomer-Resolved Measurements of Sequential Addition of Acetylene to the Propargyl Radical. *J. Phys. Chem. Lett.* **2015**, *6*, 4153–4158.
- (31) Sharma, S.; Harper, M. R.; Green, W. H. Modeling of 1,3-Hexadiene, 2,4-Hexadiene and 1,4-Hexadiene-Doped Methane Flames: Flame Modeling, Benzene and Styrene Formation. *Combust. Flame* **2010**, *157*, 1331–1345.
- (32) Mebel, A. M.; Kislov, V. V. Can the C<sub>5</sub>H<sub>5</sub> + C<sub>5</sub>H<sub>5</sub> → C<sub>10</sub>H<sub>10</sub> → C<sub>10</sub>H<sub>9</sub> + H/C<sub>10</sub>H<sub>8</sub> + H<sub>2</sub> Reaction Produce Naphthalene? An Ab Initio/RRKM Study. *J. Phys. Chem. A* **2009**, *113*, 9825–9833.
- (33) Wang, D.; Violi, A.; Kim, D. H.; Mullholland, J. A. Formation of Naphthalene, Indene, and Benzene from Cyclopentadiene Pyrolysis: A DFT Study. *J. Phys. Chem. A* **2006**, *110*, 4719–4725.
- (34) Cavallotti, C.; Polino, D. On the Kinetics of the C<sub>5</sub>H<sub>5</sub> + C<sub>5</sub>H<sub>5</sub> Reaction. *Proc. Combust. Inst.* **2013**, *34*, 557–564.
- (35) Cavallotti, C.; Polino, D.; Frassoldati, A.; Ranzi, E. Analysis of Some Reaction Pathways Active during Cyclopentadiene Pyrolysis. *J. Phys. Chem. A* **2012**, *116*, 3313–3324.
- (36) Kislov, V. V.; Mebel, A. M. The Formation of Naphthalene, Azulene, and Fulvalene from Cyclic C<sub>5</sub> Species in Combustion: An Ab Initio/RRKM Study of 9-H-Fulvalenyl (C<sub>5</sub>H<sub>5</sub>–C<sub>5</sub>H<sub>4</sub>) Radical Rearrangements. *J. Phys. Chem. A* **2007**, *111*, 9532–9543.
- (37) Benson, S. W. *Thermochemical Kinetics: Methods for the Estimation of Thermochemical Data and Rate Parameters*; Wiley: New York, NY, 1968.
- (38) Pincock, J. A.; Boyd, R. J. Thermal and Photochemical Reactivity of Cyclopropene Derivatives: a Semi-empirical Molecular Orbital Study. *Can. J. Chem.* **1977**, *55*, 2482–2491.
- (39) Billups, W. E.; Lin, L.-J. Uses of Adsorbed Reagents in the Synthesis of Reactive Molecules via Elimination Reactions. *Tetrahedron* **1986**, *42*, 1575–1579.
- (40) Bloch, R.; Le Perche, P.; Conia, J. M. Dimethylenecyclopropane. *Angew. Chem., Int. Ed. Engl.* **1970**, *9*, 798–799.
- (41) Hansen, N.; Klippenstein, S. J.; Miller, J. A.; Wang, J.; Cool, T. A.; Law, M. E.; Westmoreland, P. R.; Kasper, T.; Kohse-Höinghaus, K. Identification of C<sub>5</sub>H<sub>x</sub> Isomers in Fuel-Rich Flames by Photoionization Mass Spectrometry and Electronic Structure Calculations. *J. Phys. Chem. A* **2006**, *110*, 4376–4388.
- (42) Gong, C.-M.; Ning, H.-B.; Li, Z.-R.; Li, X.-Y. Theoretical and Kinetic Study of Reaction C<sub>2</sub>H + C<sub>3</sub>H<sub>6</sub> on the C<sub>3</sub>H<sub>7</sub> Potential Energy Surface. *Theor. Chem. Acc.* **2015**, *134*, 1599.
- (43) He, C.; Zhao, L.; Thomas, A. M.; Galimova, G. R.; Mebel, A. M.; Kaiser, R. I. A Combined Experimental and Computational Study on the Reaction Dynamics of the 1-Propynyl Radical (CH<sub>3</sub>CC; X<sup>2</sup>A<sub>1</sub>) with Ethylene (H<sub>2</sub>CCH<sub>2</sub>; X<sup>1</sup>A<sub>g</sub>) and the Formation of 1-Penten-3-yne (CH<sub>2</sub>CHCCCH<sub>3</sub>; X<sup>1</sup>A'). *Phys. Chem. Chem. Phys.* **2019**, *21*, 22308–22319.
- (44) He, C.; Zhao, L.; Doddipatla, S.; Thomas, A. M.; Nikolayev, A. A.; Galimova, G. R.; Azyazov, V. N.; Mebel, A. M.; Kaiser, R. I. Gas-Phase Synthesis of 3-Vinylcyclopropene via the Crossed Beam Reaction of the Methylidyne Radical (CH; X<sup>2</sup>Π) with 1,3-Butadiene (CH<sub>2</sub>CHCHCH<sub>2</sub>; X<sup>1</sup>A<sub>g</sub>). *ChemPhysChem* **2020**, *21*, 1295–1309.
- (45) Kaiser, R. I.; Balucani, N. The Formation of Nitriles in Hydrocarbon-Rich Atmospheres of Planets and Their Satellites: Laboratory Investigations by the Crossed Molecular Beam Technique. *Acc. Chem. Res.* **2001**, *34*, 699–706.
- (46) Guo, Y.; Gu, X.; Kawamura, E.; Kaiser, R. I. Design of a Modular and Versatile Interlock System for Ultrahigh Vacuum Machines: A Crossed Molecular Beam Setup as a Case Study. *Rev. Sci. Instrum.* **2006**, *77*, 034701.
- (47) Kaiser, R. I.; Ting, J. W.; Huang, L. C. L.; Balucani, N.; Asvany, O.; Lee, Y. T.; Chan, H.; Stranges, D.; Gee, D. A Versatile Source to Produce High-Intensity, Pulsed Supersonic Radical Beams for Crossed-Beam Experiments: The Cyanogen Radical CN (X<sup>2</sup>Σ<sup>+</sup>) as a case study. *Rev. Sci. Instrum.* **1999**, *70*, 4185–4191.
- (48) Balucani, N.; Asvany, O.; Chang, A. H. H.; Lin, S. H.; Lee, Y. T.; Kaiser, R. I.; Bettinger, H. F.; Schleyer, P. v. R.; Schaefer, H. F., III Crossed Beam Reaction of Cyano Radicals with Hydrocarbon Molecules. I. Chemical Dynamics of Cyanobenzene (C<sub>6</sub>H<sub>5</sub>CN; X<sup>1</sup>A<sub>1</sub>) and Perdeutero Cyanobenzene (C<sub>6</sub>D<sub>5</sub>CN; X<sup>1</sup>A<sub>1</sub>) Formation from Reaction of CN(X<sup>2</sup>Σ<sup>+</sup>) with Benzene C<sub>6</sub>H<sub>6</sub> (X<sup>1</sup>A<sub>g</sub>), and d<sub>6</sub>-Benzene C<sub>6</sub>D<sub>6</sub> (X<sup>1</sup>A<sub>g</sub>). *J. Chem. Phys.* **1999**, *111*, 7457–7471.
- (49) Balucani, N.; Asvany, O.; Chang, A. H. H.; Lin, S. H.; Lee, Y. T.; Kaiser, R. I.; Bettinger, H. F.; Schleyer, P. v. R.; Schaefer, H. F., III Crossed Beam Reaction of Cyano Radicals with Hydrocarbon Molecules. II. Chemical Dynamics of 1-Cyano-1-Methylallene (CNCH<sub>3</sub>CCCH<sub>2</sub>; X<sup>1</sup>A') Formation from Reaction of CN(X<sup>2</sup>Σ<sup>+</sup>) with Dimethylacetylene CH<sub>3</sub>CCCH<sub>3</sub> (X<sup>1</sup>A<sub>1</sub>'). *J. Chem. Phys.* **1999**, *111*, 7472–7479.
- (50) Jefferts, K. B.; Penzias, A. A.; Wilson, R. W. Observation of the CN Radical in the Orion Nebula and W51. *Astrophys. J.* **1970**, *161*, L87–L89.
- (51) Kaiser, R. I.; Lee, Y. T.; Suits, A. G. Crossed-Beam Reaction of C(<sup>3</sup>P) with C<sub>2</sub>H<sub>2</sub>(<sup>1</sup>Σ<sup>+</sup><sub>g</sub>): Observation of Tricarbon-Hydride C<sub>3</sub>H. *J. Chem. Phys.* **1995**, *103*, 10395–10398.
- (52) Stahl, F.; von Ragué Schleyer, P.; Bettinger, H. F.; Kaiser, R. I.; Lee, Y. T.; Schaefer, H. F., III Reaction of the Ethynyl Radical, C<sub>2</sub>H, with Methylacetylene, CH<sub>3</sub>CCH, under Single Collision Conditions: Implications for Astrochemistry. *J. Chem. Phys.* **2001**, *114*, 3476–3487.
- (53) Kaiser, R. I.; Mebel, A. M.; Lee, Y. T. Chemical Dynamics of Cyclopropynylidyne (c-C<sub>3</sub>H; X<sup>2</sup>B<sub>2</sub>) Formation from the Reaction of C(<sup>1</sup>D) with Acetylene, C<sub>2</sub>H<sub>2</sub> (X<sup>1</sup>Σ<sup>+</sup><sub>g</sub>). *J. Chem. Phys.* **2001**, *114*, 231–239.
- (54) Kaiser, R. I.; Maksyutenko, P.; Ennis, C.; Zhang, F.; Gu, X.; Krishtal, S. P.; Mebel, A. M.; Kostko, O.; Ahmed, M. Untangling the Chemical Evolution of Titan's Atmosphere and Surface—from Homogeneous to Heterogeneous Chemistry. *Faraday Discuss.* **2010**, *147*, 429–478.
- (55) Thomas, A. M.; Zhao, L.; He, C.; Galimova, G. R.; Mebel, A. M.; Kaiser, R. I. Directed Gas-Phase Synthesis of Trifulvene under Single-Collision Conditions. *Angew. Chem., Int. Ed.* **2019**, *58*, 15488–15495.
- (56) He, C.; Thomas, A. M.; Galimova, G. R.; Mebel, A. M.; Kaiser, R. I. Gas-Phase Formation of 1-Methylcyclopropene and 3-Methylcyclopropene via the Reaction of the Methylidyne Radical (CH; X<sup>2</sup>Π) with Propylene (CH<sub>3</sub>CHCH<sub>2</sub>; X<sup>1</sup>A'). *J. Phys. Chem. A* **2019**, *123*, 10543–10555.
- (57) Brink, G. O. Electron Bombardment Molecular Beam Detector. *Rev. Sci. Instrum.* **1966**, *37*, 857–860.
- (58) Daly, N. R. Scintillation Type Mass Spectrometer Ion Detector. *Rev. Sci. Instrum.* **1960**, *31*, 264–267.
- (59) Kaiser, R. I.; Lee, Y. T.; Suits, A. G. Crossed-beam Reaction of Carbon Atoms with Hydrocarbon Molecules. I. Chemical Dynamics of the Propargyl Radical Formation, C<sub>3</sub>H<sub>3</sub> (X<sup>2</sup>B<sub>2</sub>), from Reaction of

C(<sup>3</sup>P) with Ethylene, C<sub>2</sub>H<sub>4</sub>(X<sup>1</sup>A<sub>g</sub>). *J. Chem. Phys.* **1996**, *105*, 8705–8720.

(60) Kaiser, R. I.; Stranges, D.; Lee, Y. T.; Suits, A. G. Crossed-beam Reaction of Carbon Atoms with Hydrocarbon Molecules. II. Chemical Dynamics of n-C<sub>4</sub>H<sub>3</sub> Formation from Reaction of C(<sup>3</sup>P) with Methylacetylene, CH<sub>3</sub>CCH (X<sup>1</sup>A<sub>1</sub>). *J. Chem. Phys.* **1996**, *105*, 8721–8733.

(61) Weiss, P. S. *The Reactions of Ground and Excited State Sodium Atoms with Hydrogen Halide Molecules*. Ph. D. Dissertation Thesis, University of California: Berkeley, CA, 1986.

(62) Vernon, M. F. *Molecular Beam Scattering*. Ph.D. Dissertation Thesis, University of California: Berkeley, CA, 1983.

(63) Kaiser, R. I.; Ochsenfeld, C.; Stranges, D.; Head-Gordon, M.; Lee, Y. T. Combined Crossed Molecular Beams and *Ab Initio* Investigation of the Formation of Carbon-bearing Molecules in the Interstellar Medium via Neutral–Neutral Reactions. *Faraday Discuss.* **1998**, *109*, 183–204.

(64) Gu, X.; Guo, Y.; Zhang, F.; Mebel, A. M.; Kaiser, R. I. Reaction Dynamics of Carbon-bearing Radicals in Circumstellar Envelopes of Carbon Stars. *Faraday Discuss.* **2006**, *133*, 245–275.

(65) Mebel, A. M.; Kaiser, R. I. Formation of Resonantly Stabilised Free Radicals via the Reactions of Atomic Carbon, Dicarbon, and Tricarbon with Unsaturated Hydrocarbons: Theory and Crossed Molecular Beams Experiments. *Int. Rev. Phys. Chem.* **2015**, *34*, 461–514.

(66) Becke, A. D. Density-Functional Thermochemistry. III. The Role of Exact Exchange. *J. Chem. Phys.* **1993**, *98*, 5648–5652.

(67) Lee, C.; Yang, W.; Parr, R. G. Development of the Colle-Salvetti Correlation-Energy Formula into a Functional of the Electron Density. *Phys. Rev. B: Condens. Matter Mater. Phys.* **1988**, *37*, 785–789.

(68) Adler, T. B.; Knizia, G.; Werner, H.-J. A Simple and Efficient CCSD(T)-F12 Approximation. *J. Chem. Phys.* **2007**, *127*, 221106.

(69) Knizia, G.; Adler, T. B.; Werner, H.-J. Simplified CCSD(T)-F12 Methods: Theory and Benchmarks. *J. Chem. Phys.* **2009**, *130*, 054104.

(70) Werner, H.-J.; Knowles, P. J.; Lindh, R.; Manby, F. R.; Schütz, M.; Celani, P.; Korona, T.; Rauhut, G.; Amos, R. D.; Bernhardsson, A. *MOLPRO, Version 2010.1, A Package of Ab Initio Programs*; University of Cardiff: Cardiff, U.K., 2010.

(71) Dunning, T. H., Jr Gaussian Basis Sets for Use in Correlated Molecular Calculations. I. The Atoms Boron through Neon and Hydrogen. *J. Chem. Phys.* **1989**, *90*, 1007–1023.

(72) Zhang, J.; Valeev, E. F. Prediction of Reaction Barriers and Thermochemical Properties with Explicitly Correlated Coupled-cluster Methods: a Basis Set Assessment. *J. Chem. Theory Comput.* **2012**, *8*, 3175–3186.

(73) Frisch, M. J.; Trucks, G. W.; Schlegel, H. B.; Scuseria, G. E.; Robb, M. A.; Cheeseman, J. R.; Scalmani, G.; Barone, V.; Mennucci, B.; Petersson, G. A.; et al. *Gaussian 09*, Rev. A.1; Gaussian Inc.: Wallingford, CT, 2009.

(74) Steinfeld, J. I.; Francisco, J. S.; Hase, W. L. *Chemical Kinetics and Dynamics*. Prentice Hall: Englewood Cliffs, NJ, 1982; Vol. 3.

(75) Eyring, H.; Lin, S. H.; Lin, S. M. *Basic Chemical Kinetics*; John Wiley and Sons, Inc.: New York, 1980.

(76) Robinson, P. J.; Holbrook, K. A. *Unimolecular Reactions*; Wiley: New York, 1972.

(77) He, C.; Zhao, L.; Thomas, A. M.; Morozov, A. N.; Mebel, A. M.; Kaiser, R. I. Elucidating the Chemical Dynamics of the Elementary Reactions of the 1-Propynyl Radical (CH<sub>3</sub>CC; X<sup>2</sup>A<sub>1</sub>) with Methylacetylene (H<sub>3</sub>CCCH; X<sup>1</sup>A<sub>1</sub>) and Allene (H<sub>2</sub>CCCH<sub>2</sub>; X<sup>1</sup>A<sub>1</sub>). *J. Phys. Chem. A* **2019**, *123*, 5446–5462.

(78) Kislov, V. V.; Nguyen, T. L.; Mebel, A. M.; Lin, S. H.; Smith, S. C. Photodissociation of Benzene under Collision-free Conditions: An *Ab Initio*/Rice–Ramsperger–Kassel–Marcus Study. *J. Chem. Phys.* **2004**, *120*, 7008–7017.

(79) Levine, R. D.; Bernstein, R. B.; Lee, Y. T. Molecular Reaction Dynamics and Chemical Reactivity. *Phys. Today* **1988**, *41*, 90–92.

(80) Levine, R. D. *Molecular Reaction Dynamics*; Cambridge University Press: Cambridge, U.K., 2005.

(81) Herschbach, D. R. Reactive Collisions in Crossed Molecular Beams. *Discuss. Faraday Soc.* **1962**, *33*, 149–161.

(82) Miller, W. B.; Safron, S. A.; Herschbach, D. R. Exchange Reactions of Alkali Atoms with Alkali Halides: A Collision Complex Mechanism. *Discuss. Faraday Soc.* **1967**, *44*, 108–122.

(83) Djokic, M. R.; Van Geem, K. M.; Cavallotti, C.; Frassoldati, A.; Ranzi, E.; Marin, G. B. An Experimental and Kinetic Modeling Study of Cyclopentadiene Pyrolysis: First Growth of Polycyclic Aromatic Hydrocarbons. *Combust. Flame* **2014**, *161*, 2739–2751.